Design And Analysis Of Microwave Bootlace Lens

Thesis

Submitted for the degree of

Doctor Of Philosophy

In

Electronics & communication Engineering

To

Bundelkhand University

Jhansi(UP)

By

D.C. Dhubkarya
Electronis & Communiaction Engg. Department
B.I.E.T. Jhansi 284125(UP)

India-2008

CERTIFICATE

This is to certify that the thesis entitled "**Design and analysis of microwave bootlace lens**" submitted to the Bundelkhand University Jhansi (U.P.) India for the award of degree of doctor of philosophy in electronics and communication engineering is a record of bonafide research work carried out by **D.C.Dhubkarya** under our guidance and supervision.

The work embodied in this thesis or a part were of has not been submitted for the award of any other degree. He has completed 200 hr at Study Centre.

Supervisors

17/3/08

Prof. R.C.Saraswat,
Vice-Chancellor
Veer Bahadur Singh Purvanchal University,Jaunpur
and Ex. Director, B.I.E.T. Jhansi

Prof.P.K.Singhal
Prof. [illegible]
Electronics & Comm. Engg. Department
M.I.T.S., Gwalior

DECLARATION

I here by declare that the work presented in this thesis **"Design and Analysis of Microwave Bootlace Lens"** is entirely my own work and there are no collaborators. It does not contain any work for which any other university has awarded degree.

(D C DHUBKARYA)

Countersigned

Supervisor

Prof. R.C.Saraswat,
Vice-Chancellor
Veer Bahadur Singh Purvanchal University,Jaunpur
and Ex. Director, B.I.E.T. Jhansi

17/3/05
Prof.P.K.Singhal
Prof.
Electronics & Comm. Engg. Department
M.I.T.S., Gwalior

Acknowledgements

I feel greatly privileged in offering my sincere thanks and expressing deepest sense of gratitude and profound respects to my thesis supervisors **Prof. R.C.Saraswat** and **Prof. P.K.Singhal** for his valuable guidance, constant encouragement, stimulating advise instructuctive and fruitful suggestions and above all significant contribution made by him, through out my research work of Ph.D. without which this work could not have taken the present form. He always instilled in me a sprit of confidence and independent thinking and evaluation in the course of the investigation and preparation of the manuscript. I have all praise for him and will always go holding him in high esteem even throughout my educational career.

I don't have any appropriate words to express my heartiest thanks and gratitude to Prof. S.K.Awasthi, Director Bundelkhand institute of Engineering and technology, Jhansi for his constant encouragement and moral support throughout my research work.

I express my thanks to Er. Mahendra Kumar, Er. Vishal Nagar, Shri A.K.Saraogi and all staff member of Electronics & Communication Engineering department.

On this occasion, I sincere thanks to my parents & all family members, I cannot forget to pay my sincere thanks to my beloved wife Mrs.Deepali and my children Divyansh & Divyasha for their constant encouragement and patience during this time consuming work.

D.C.Dhubkarya

INDEX

CHAPTER ONE

INTRODUCTION

In radar and communication applications it is required to generate multiple beams using an antenna array. A multiple beam forming network is required to control the amplitude and phase at each element of the antenna array. Microwave lenses form an important class of multiple beam forming networks.

This chapter describes the review of work reported so far for design and analysis of multiple beams forming bootlace lens. An outline of the thesis is also given.

1.1 MULTIPLE BEAM FORMING NETWORK AND LENS

In many radar and communication applications, it is necessary to scan a wide area. Parabolic reflector antenna is most commonly used for this purpose as shown in figure 1.1. However, this arrangement has major disadvantage:

1. Difficult to realize large aperture due to mechanical constraints like back up structure and gears.

2. Blockage by the feed structure.

3. Slow in response as related to scanning in comparison to electronics scanning, suffers reliability problem from shock and vibration.

4. Due to edging, angle of coupling and other mechanical disorders.

An antenna array with multiple beams forming network as shown in figure1.2 can be used as an alternative to parabolic reflector antenna. The multiple beam forming network is used to control the amplitude and phase at each element of the antenna array. Two types of multiple beam forming networks are available:

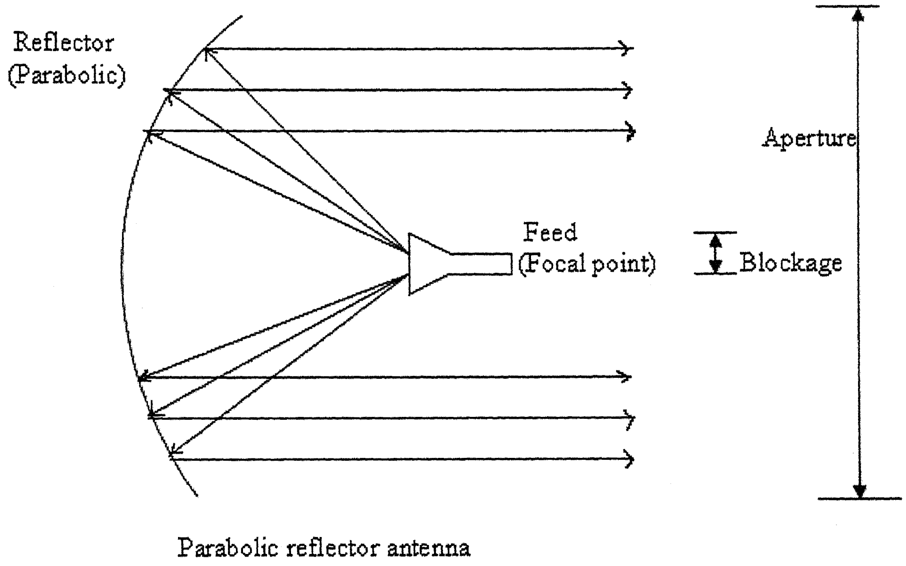

FIGURE 1.1 PARABOLIC REFLECTOR ANTENNA

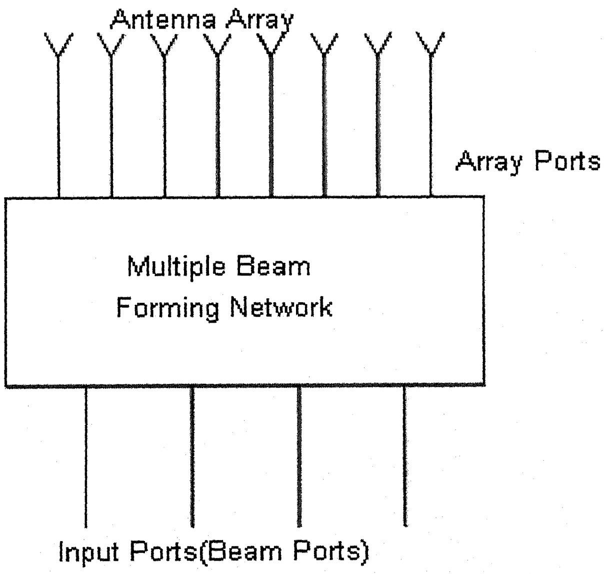

FIGURE 1.2 ANTENNA ARRAY WITH MULTIPLE BEAMS FORMING NETWORK

1. Circuit type multiple beam forming network.

2. Microwave bootlace lens.

The circuit type multiple beam forming network [1] as shown in figure 1.3 consisting number of directional coupler, phase shifter, power divider, cross-over etc. Phase shifters are costly to fabricate and introduce considerable RF losses. For large number of input-output ports this design becomes extremely complicated. Microwave bootlace lens suggested by Rotman and Turner [2] is a useful alternative to this complicated circuit type multiple beam forming network. This design was further corrected by D.Larry Leonakis [3].

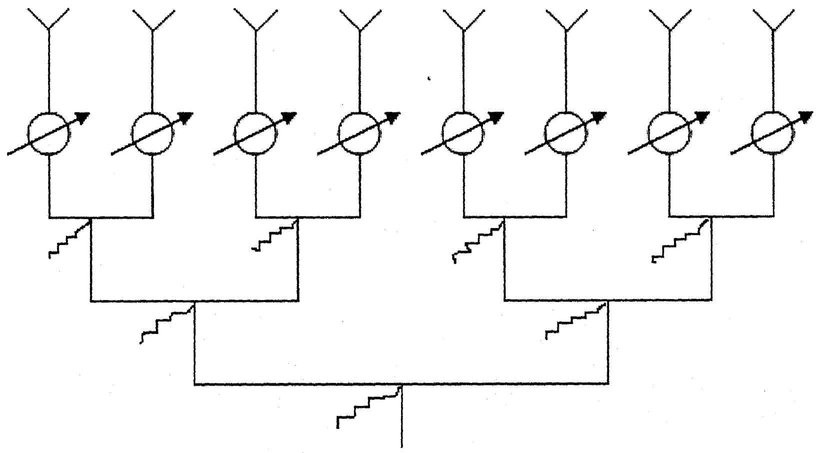

FIGURE 1.3 CIRCUIT TYPE MULTIPLE BEAM FORMING NETWORK

A microwave lens is basically a phase corrective device, which transforms a divergent wave front from a point source into a plane wave. A microwave lens usually consists of two surfaces, one being the pickup surface and the other is the radiating surface. Microwave lenses can be broadly divided into two categories [4].

1. Dielectric lens
2. Constrained lens

A dielectric lens is made of dielectric material. It obeys Snell's law and works as an optical lens as shown in figure 1.4. Such lenses are also called 'normal' lenses [4].

In a constrained lens, metal plates guide a wave to follow a particular path as shown in figure 1.5. Obviously such lenses do not obey Snell's law and the direction of outgoing beam is not affected by the refractive index of the medium. The lens consists of parallel plate with plate separation less than $\lambda/2$, where λ is wavelength of the operating frequency, so only TEM mode can propagate. A constrained lens can be defined as any microwave-transforming device in which the wave is guided to follow a certain discrete path. Path lengths and geometries of these guiding components are so adjusted that the lens produces the desired output phase and amplitude distribution. Constrained lenses may be designed to provide multiple foci for wide-angle scanning.

First of all Ruze [4] suggested a constrained lens for wide angle scanning. Figure 1.6 shows the lens configuration suggested by Ruze. This lens has elliptical output contour and two focal points (O and O′) located on a circular arc. The lens is designed in such a way that a plane wave is radiated at an angle α when the source is placed at point O, and at an angle $-\alpha$ when the source is placed at point O′. For the desired plane wave, it is required

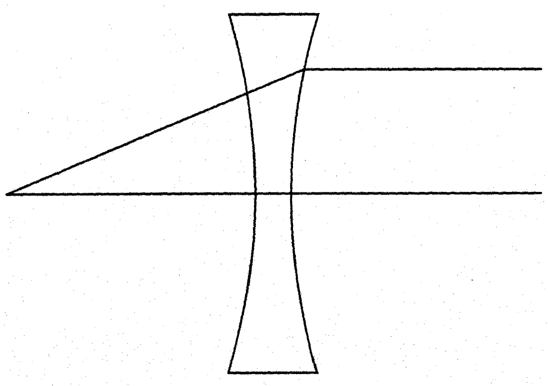

FIGURE 1.4 DIELECTRIC LENS

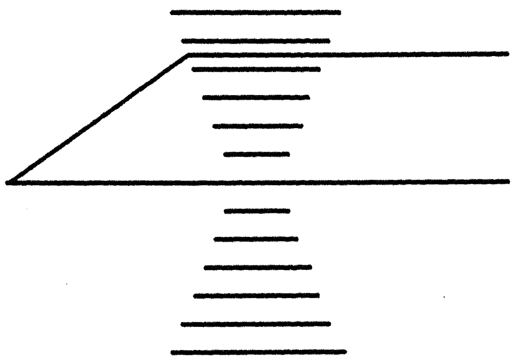

FIGURE 1.5 CONSTRAINED LENS

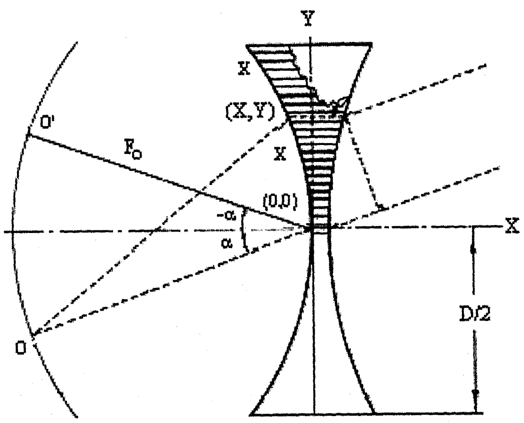

FIGURE 1.6 LENS GEOMETRY SUGGESTED BY RUZE

that the phase or electrical path length difference between a general ray and a central ray be zero or integral multiple of a wavelength.

A constrained lens usually consists of a number of receiving and radiating elements on each surface of the lens. Input and radiating elements are connected to the lens by TEM mode transmission lines as shown in figure 1.7. Excitation at each input produces a suitable phase and amplitude distribution across the array element so as to produce beam in a particular direction. Figure 1.7 shows the direction of outgoing beam for input at different

feed points. A lens input ports are also called beam ports and output ports are also called array ports.

Rotman and Turner [2] suggested modifications in Ruze's constrained lens, to improve the scanning capabilities.

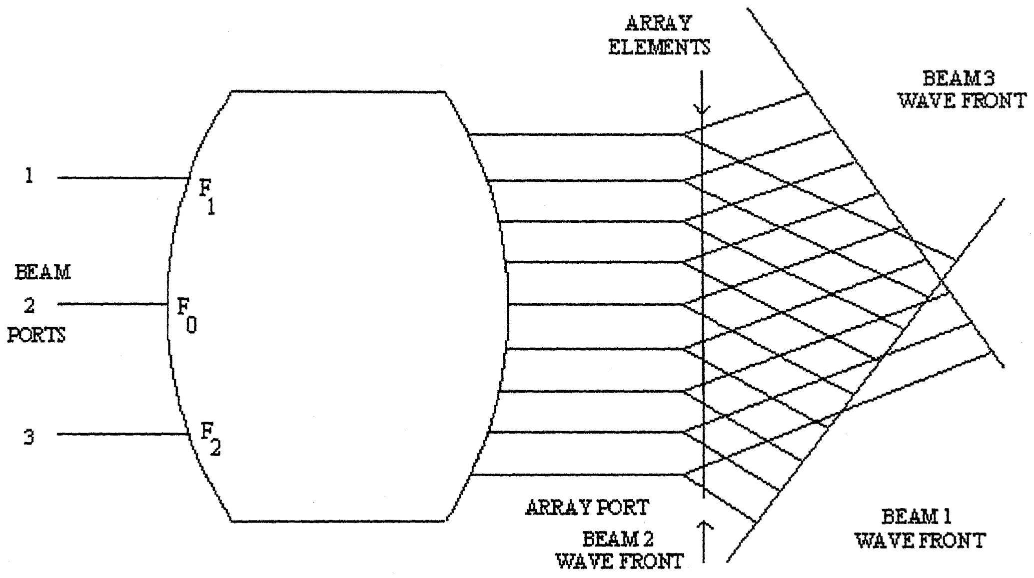

FIGURE 1.7 LINEAR ARRAY FED BY CONSTRAINED LENS

1.2 THE ROTMAN LENS

Figure 1.8 shows the cross-section of a trifocal Rotman lens. One focal point F_o is located on the central axis of the lens and two other (F_1 and F_2) are symmetrically located on either side of the axis of the lens at focal angles $\pm\ \alpha$ on a circular focal arc. Focal arc is also called beam contour or feed contour. Antenna array elements are located on a straight line I_2 (called lens aperture). I_1 is the inner contour of the lens also called array contour. Radiating elements and array contour are connected by TEM mode transmission lines W (N). This gives the appearance of an untightened bootlace, hence this type of lens is also called bootlace lens.

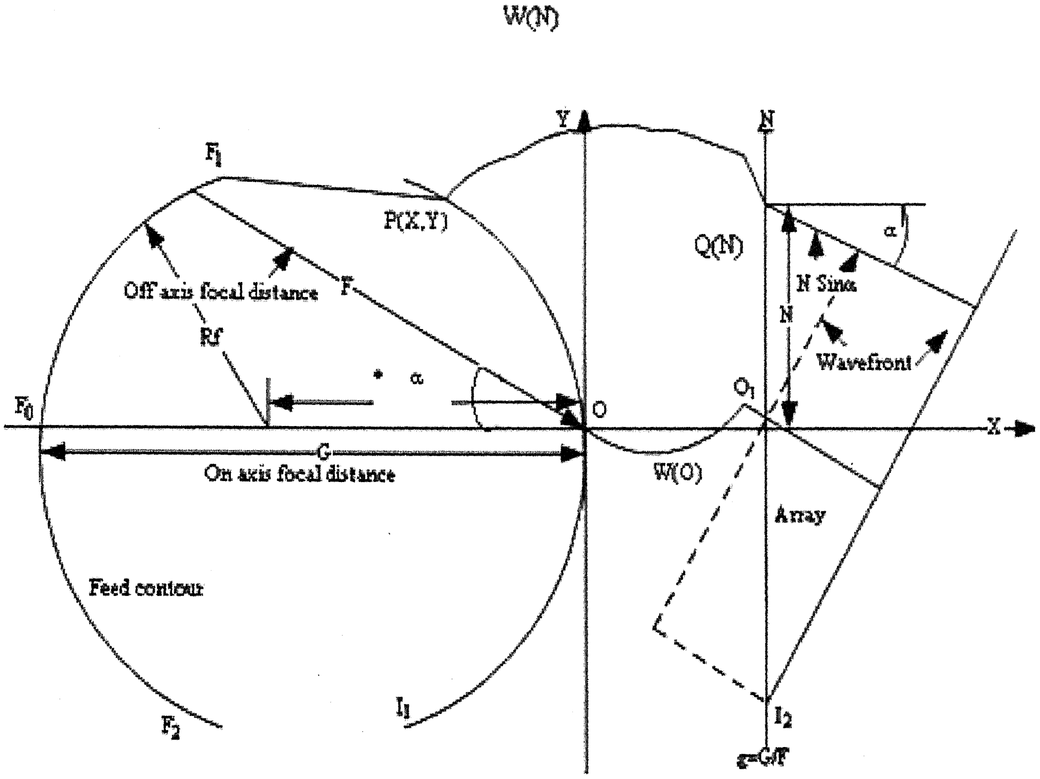

FIGURE 1.8: CROSSSECTION OF ROTMAN LENS

The array contour I_1 is defined by coordinates (X, Y). The position of the radiating elements on the straight line I_2 are determined by single coordinate N, measured relative to point O_1. Points O_1 and O lie on the contours I_2 and I_1 respectively and connected by transmission line of length W(O). A general point P(X, Y) on the array contour is connected to element Q (N) which lies on I_2 by the transmission line of length W (N).

This new lens design differs from the Ruze model where corresponding points on the two lens counters (I_1 and I_2) are not equidistant from the central axis. This change is made by introducing flexible transmission lines between lens's inner contours and radiating elements. In Rotman lens, four basic parameters are selected: Straight front face, two symmetrical off axis focal points and an on axis focal point. Array contours and

transmission lines are designed in such a way that the outgoing beam makes an angle - α, 0 and α with the axis of the lens and terminates normal to their respective wave-front, when feed point is placed at F_1, F_0, and F_2 respectively. The orientation of wave front for each focal point is shown in figure 1.7.

A ray originating from point F_1 on the feed contour may reach the wave-front through a general point P (X, Y) on the array contour, transmission line W (N), point Q (N) and then tracing a straight line at an angle -α. Also the ray may reach the wave front from F_1 to O, transmission line W (O) and terminates normal to the wave front. Similarly rays from F_2 and F_0 may reach their respective wave fronts. At the wave front all the rays must be in a phase independent of the path they traveled. The lens can be designed by optical path length comparison such that the path length from the focal point to any point on the corresponding wave front is constant [2-4].

Wide-angle scanning capabilities of these lenses are described in [5-6]. Lenses of this type in principle are wide band systems since their design is based upon optical path length comparison. However their bandwidth is limited by many elements used with the lens such as properties of array elements, connecting transmission lines, the array geometry and mutual coupling effect. Bandwidth for a given lens must be defined carefully in terms of array performance. The definition of bandwidth from different points of view has been examined and summarized by Frank [7].

1.3 PHASE ERROR (PATH LENGTH ERROR)

The Rotman lens discussed above is a lens with three focal points located at angles 0 and $\pm$ α on the focal arc. When a feed is placed at one of these focal points corresponding emitted wave front has no phase error, since the condition of constant path length is satisfied. When the feed is displaced from these focal points, the corresponding wave front will have phase error. However, for wide angle scanning lens must focus at all the

intermediate points along the focal arc. Ruze [4] derived the phase error as power series across the lens aperture, as

$$\delta L = ay + by^2 + cy^3 + \ldots\ldots\ldots\ldots\ldots\ldots \qquad (1.1)$$

Where the constants a, b, c, ----- are functions of the feed position, and the parameters of the lens and 'y' is the Y-coordinate of the outer contour of the lens. These constants must be zero at the point of perfect focus. Nature of the series and the magnitude of the various terms will determine the type of distortion. The first term of the series represents a linear phase variation and therefore a tilting without distortion of the radiation. The second order term yields a radiation pattern equivalent to the "close in" pattern of an aperture with a uniform phase. The cubic term yields a third order aberration known as "Coma". Higher order terms exist and their aggregate forms a significant contribution to the total phase error especially at large angles. However such terms are individually smaller than the coma term.

Refocusing the focal arc may eliminate the second order aberration. Refocusing consists of moving the feed radially to a point where the best patterns are obtained. Figure 1.9 shows how focal arc is suitably modified to reduce the phase error. However even after refocusing the focal arc, objectionable phase error is present.

Katagi and others [8] defined the following equation for minimization of phase error

$$\varepsilon = \int_{-1}^{1} \delta L dn \qquad (1.2)$$

Value of path length error δL is substituted in the above equation and coordinates of the focal arc are determined for minimum value of ε. In [8] it was shown that phase error (path length error) is considerably reduced by refocusing the focal arc according to the above equation.

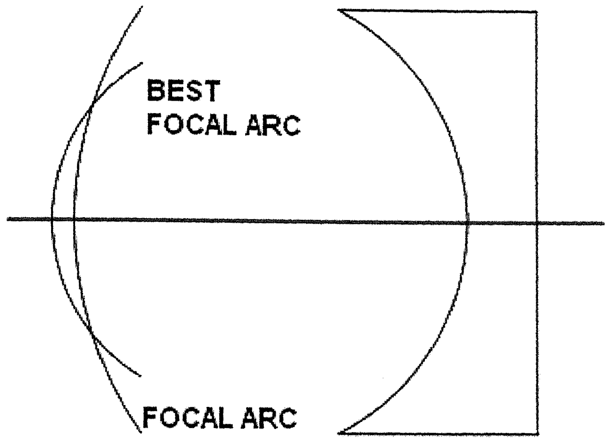

FIGURE 1.9 REFOCUSING OF THE FOCAL ARC

1.4 MODIFICATIONS PROPOSED IN ROTMAN LENS

Rotman and turner required that the feed curve be circular and they optimized the design parameters accordingly. These types of lens are wide band systems. Since design is based on the different optical path length comparison. However, their bandwidth is dependent on the circuit elements used for the realization of the lenses such as: array elements, connecting TEM transmission lines, the array geometries and mutual coupling effects.

Shelton [9] suggested modification in the design and stated that it is not necessary to have circular focal arc and a lens with front-to-back symmetry was designed. In this design input ports and array ports can be interchanged. The reasons for choosing symmetrical configuration are:

1. An asymmetrical lens will have either the lens arc or the feed arc more strongly curved than the arcs obtained for the symmetric solution. The more curved arc will have larger port spacing and a larger variation in port spacing from the centre to the edge.
2. Symmetric lens exhibits better aberration characteristics.

3. The tendency for feed ports to illuminate other feed ports is more severe for asymmetric lens.
4. The symmetric lens is smaller than an equivalent asymmetric lens.

Smith [10] used conventional geometrical optics approach to analyze the Ruze and Rotman lenses and extended the approach in two ways. Firstly, the path length formulae are expanded as a power series, bringing out the wanted linear phase variation plus the higher order phase aberration terms. These are given explicitly in terms of lens parameters to find the lens contour such that second and third order aberrations are zero. The second analysis is of the variation of lens performance with its dimension G (the central distance between input and output contours). A relation for minimum value of 'G' required for given array length and scanning angle was derived.

M.J. Gans *et.al* [11] have designed a dual polarized narrow beam antenna to use for geostationary arc coverage of 60°. The beam width is less than 0.5°. It produces conically scanned beam by means of linear array of feed horns with bias cut apertures illuminating a pair of parabolic cylinder reflector in a special arrangement of images. This design is relatively simple because it uses reduced size array and singly curved reflector.

J.S. Herd *et.al* [12] have designed and fabricated an eight microstrip antenna array feed by a microstrip Rotman lens. The method of moment was used to find the feed point optimization which is more accurate. Microstrip Rotman lens is fabricated for broad band multiple beam feed. It has been found that feed point optimization by means of a method of moments solution is highly accurate, and that the microstrip Rotman lens was an inexpensive fabricated broadband multiple beam feed structure.

Rappaport *et.al* [13] have designed three dimensional bifocal and quadrufocal bootlace lenses using curved focal arc. Due to availability of curved focal arc, for three dimensional bifocal and quadrufocal bootlace lenses. This design is difficult but reliable, compact and having low insertion loss.

H.L. Southall *et.al* [14] have designed, fabricated and tested a completely overlapped sub array antenna for broad band, low side lobes and wide scan angle performance. It used time delay steering at the inputs to a transformed feed, which illuminates a phase shifter steered objective lens.

D.L. Johnson *et.al* [15] have designed an offset pillbox reflector with a 2^0 maximum H- plane -3 dB beam width and -35 dB maximum side lobes over a 6 GHz to 12 GHz band. The linear array of 23 elements is primary feed for offset reflector.

L. Musa *et.al* [16,17] have designed a microstrip Rotman lens port. In this design a microstrip port is viewed as a 2-D aperture antenna. An open ended waveguide radiator can be used having a cut angle end for beam deflection to a position between the aperture normal and the direction of the waveguide sides. In this design a cut angle microstrip port is assumed and might produce a deflection from the aperture normal to the direction defined by the guide sides.

David R. Gagnan [18] presented an alternative approach to design the lens by refocusing the focal arc according to the Snell's law and termed the new lens as refracting lens. It was designed in microstrip configuration. This approach provides beam ports and array ports placements, which gives improved coupling to the outermost beam ports, particularly for stripline or microstrip configuration used with small array antennas.

M.C.D. Maddocks *et.al* [19] have designed a flat plate steerable antenna for satellite communication and broadcast reception. They given two implementation of the Rotman lens:

1. Use a multi port lens and
2. Parallel plate lens with a single movable beam port.

KK Chan *et.al* [20] presented a simple and compact network scheme for feeding hexagonal shape planar array to produce multiple beams. Linear multiple beam forming networks are directly connected row-wise and then column-wise in an egg-crate fashion to

feed the array. All the linear networks are identical which is advantageous for low-cost implementation.

R.C. Hansen [21] has designed Rotman lens by using seven basic design parameters; focal angle, focal ratio, beam angle ratio, maximum beam angle, beam port curve ellipticity, array element spacing and focal length/λ. The advantage of beam port shaping is used to reduce phase error.

L.K. Jalalian *et.al* [22] has investigated a new concept for a frequency channelizer. This channelizer used dispersive lines to simulate the signal arriving at a given angle on a linear array. To improve the focusing properties of the Rotman lens, use low loss material with high permittivity, which reduce the size of the channelizer.

S.P.Peik et.al [23] have developed multiple beam microstrip array fed by a Rotman lens, which exhibits five independent scanned beams so that each traffic lane can be covered with only one multiple beam antenna.

Katagi *et.al* [8,24] suggested an improved design method of Rotman lens in which a new design variable is introduced and the phase error on the aperture of the antenna array is minimized. By introducing a design variable, relationship between design parameters for realizing a Rotman lens is derived and this improved method make a possible to design small and low loss Rotman lens antenna.

J.J. Lee *et.al* [25] have proposed RF heterodyne technique for Rotman lens to reduce the size of beam forming network. This design was proposed for airborne antenna operating in L-band of frequency range. The Rotman lens with 48 output ports and 60 input ports is chosen as base line approach for proposed design. The Rotman lens can be designed to have a single focal point or multiple focal points, which depends on area to be scanned, level of side lobes and phase arrays.

Y.M. Tao *et.al* [26] designed the printed circuit lens fed multiple beam antenna arrays for millimeter wave indoor personal communication systems, which is formed by a

linear array of equally spaced elements fed with an improved printed circuit Rotman lens. Both the lens and the array are designed and built on the same dielectric substrate. The antenna operates in the frequency range of 27-30 GHz and covers an angular sector near to 120° with 11 beams. The lens was implemented with wave-guide technology to minimize losses in the millimeter wave region.

E.O. Rausch *et.al* [27-29] have developed a millimeter wave Rotman lens that operates at frequencies between 33 GHz and 37 GHz. It is electronically scanned millimeter wave Rotman lens design. The various lens design were evaluated with a computer model passed on the contour integral method.

P. Phu *et.al* [30] have developed a wide bandwidth electronic scanning antenna (ESA) which is based on a Rotman lens beam forming network with shared aperture. It allows multiple beams to transmit simultaneously in different directions and at different frequencies. This design supports high bandwidth from 8 to 18 GHz frequency band.

P.K.Singhal *et.al* [31] suggest an approach to design Rotman type lens, in which height of feed and array contours was equalized to couple the maximum power from feed contour to array contour.

1.5. ANALYSIS APPROACHES OF BOOTLACE LENS

A conventional ray optics design of multiple beam forming networks gives information about the phase distribution at antenna array elements. It does not give information about the amplitude distribution at the array elements and radiation pattern of the array elements.

Smith and Fong [32] developed a theoretical model using two dimensional aperture theories to predict the amplitude performance across array ports, and insertion loss of the lens. The theoretical model treats the lens beam ports and array ports as two dimensional as shown in figure 1.10. Aperture theory is used for the flared waveguide case and would also be appropriate for a microstrip lens. A two dimensional equivalent of Friis transmission formula is derived to calculate the power received by each array port if a beam port transmits. Summing these powers allows calculating the insertion loss of the lens. The amplitude distribution is used with the phase calculated from the geometrical path length approach to predict the radiation patterns of lens fed array at various frequencies, lenses using waveguide fed parallel plate cavity and microstrip configuration were also designed. It was found experimental results are reasonable agreement with theoretical predicted result however there were differences between theoretical and experimental results. The differences can be explained in terms of multiple reflections between beam ports and array port contours.

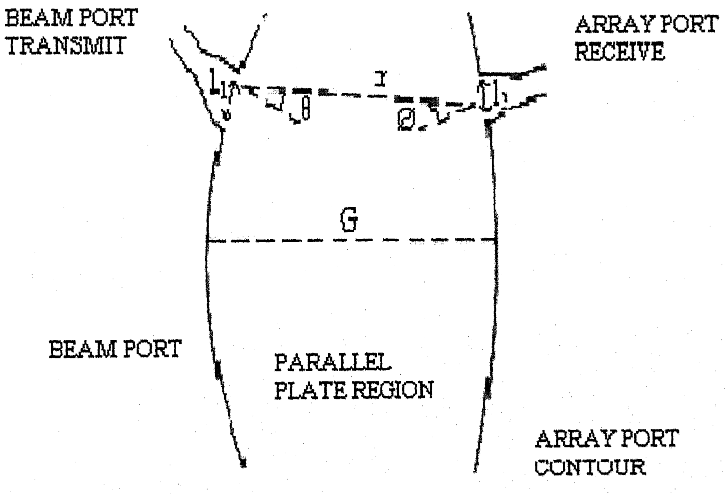

FIGURE 1.10 FEED AND ARRAY PORTS AS TWO DIMENSIONAL ANTENNAS

Design approach discussed so far does not incorporate:

1. Effects of mutual coupling between the ports.
2. Multiple scattering between feed and array contour and
3. Discontinuity reactance at junction between the lens and the transmission lines at input –output ports.

Thus the theoretical performance predicted may be significantly altered by these factors.

Fields analysis of this type of lens has not been reported extensively in the literature. In the only published studies available [33] the field distribution at port apertures, around the lens periphery is described by a contour integral solution of the wave equation using the method of moments.

P.C.Sharma et.al [34,35] reported an alternative two–dimensional field analysis approach to analyse Rotman lens. S-matrix is evaluated from the Z-matrix. A radiation pattern for the antenna array is computed using the field distribution. Analytical and experimental results were found good agreement.

1.6 LENS AS A PLANAR CIRCUIT

Rotman lens geometry in microstrip configuration is shown in figure 1.11. In microstrip or striplines configuration, height (thickness) of the lens is much smaller than the wavelength at the operating frequency and consequently, there is no variation of the field along the height of the substrate. This type of planar circuit may be considered as two-dimensional (2-d) circuit since its dimensions are comparable to the wavelength in two dimensions, but much less thickness in one direction.

Three types of such planar two- dimensional circuits are possible [36] namely.

1 Tri plate or stripline type as shown in figure. 1.12 (a)

2 Open or microstrip type as shown in figure. 1.12(b)

3 Wave guide or cavity type as shown in figure. 1.12(c)

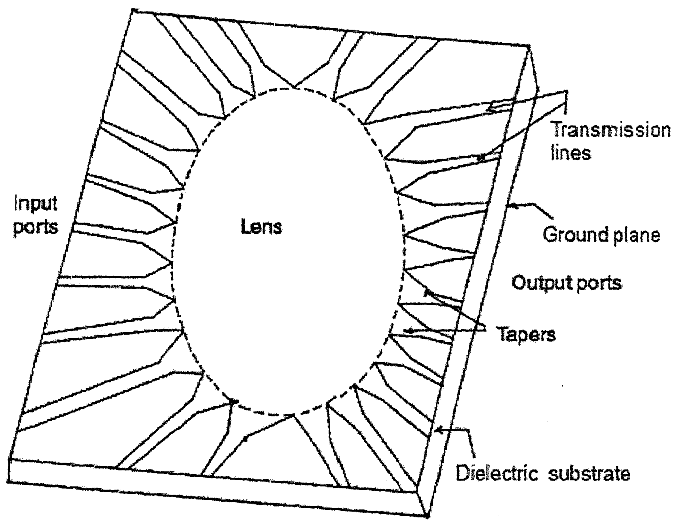

FIGURE 1.11 LENS GEOMETRY IN MICRO STRIP CONFIGURATION

The microstrip and stripline types of circuit find applications in microwave integrated circuits (MICs) and can be considered as generalization of respective one-dimensional circuits when the transverse dimension becomes comparable to the wavelength at the frequency of operation. The waveguide type circuit shown in figure 1.12(c) can be regarded as a special case of three dimensional waveguide circuit where the height is much less than the wavelength.

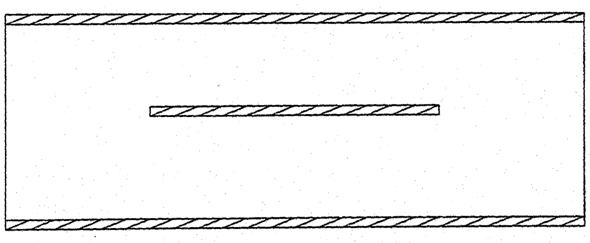

FIGURE 1.12(a) STRIPLINE TYPE PLANAR CIRCUIT

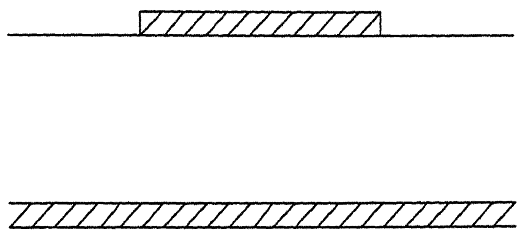

FIGURE 1.12(b) MICROSTRIP TYPE PLANAR CIRCUIT

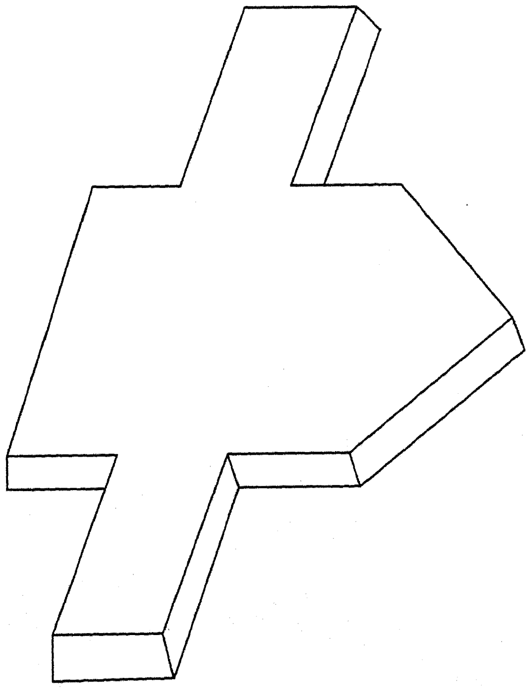

FIGURE 1.12(c) CAVITY TYPE PLANAR CIRCUIT

1.7 METHODS FOR ANALYSIS OF PLANAR CIRCUIT

The geometry of two dimensional components (i.e. the shape of the central conducting patch in a tri plate structure or the upper conducting patch in microstrip type circuit) governs the choice of the method of analysis. A brief review of various methods of analysis of two-dimensional (2-d) components is given below;

1.7.1 SPECTRAL DOMAIN ANALYSIS [37-38]

This technique has been used for quasi-static as well as for full wave analysis of some of the 2-d configuration. In quasi static approach, the capacitance for the circuit is evaluated by solving the Poisson's equation in the Fourier transform domain. In full wave analysis, Galerkin's procedure is employed to deduce a determinant characteristic equation from the coupled algebraic equations in the Fourier transform domain.

1.7.2 GREEN'S FUNCTION APPROACH

When the component or segment is of simple (regular) shape, the impedance Green's function [36] technique is the most appropriate method. Green's functions for shapes such as rectangular [36], Circular [39], right-angled isosceles triangle, equilateral triangle, 30-60° triangle [40] and for circular sectors, annular sectors and annular rings [41] are available. The impedance matrix of 2-d elements with specified locations of ports can be found using these Green's functions.

1.7.3 FINITE ELEMENTS AND CONTOUR INTEGRAL TECHNIQUES

Contour integration [42] and finite element techniques [43] have been employed for analyzing 2-d component of arbitrary geometries. In finite element method the conducting patch is divided into several segments and certain basic functions are integrated over each of these segments.

The contour integration approach [42] has been specifically proposed for 2-d component analysis and is based on Green's theorem in cylindrical co-ordinates. In this approach the voltage at a point on the periphery is evaluated in terms of a line integral along the periphery.

Rotman lens geometry in microstrip configuration as shown in figure 1.11 is an arbitrary shaped geometry. Analysis of this geometry using contour integration approach is discussed in the following chapters.

1.8 OUTLINE OF THESIS

As it is evident from the literature described so far that considerable work has not been made toward the field analysis of the lens, in the present work two-dimensional electromagnetic field analysis of Rotman lens has been carried out. Software has been used to design and analyze the lens. The results obtained for all the geometries have been compared and the lens parameters have been chosen with an intention to produce the desired response. Guidelines to select the lens design parameters have been described. Efforts have been made to reduce the design complexities and losses. The whole work has been divided in the five chapters as follows:

1. First chapter deals with a brief introduction of Rotman type multiple beam forming lens and the work done so far on the design and analysis of Rotman type lens.
2. Second chapter describes design of Rotman lens, effects of design parameters on the shape of the lens and on the performance of the lens. Guidelines to select the design parameters have been given.
3. The result of Katagi approach and others results has been compared.
4. Chapter four describes the design of Rotman type multiple beam forming lens having elliptical refocussed. The performance of new design lens has been compared with Rotman Lens.
5. The work done on Rotman type lens so far as described from chapter 1 to 4 has been concluded in chapter 5.

CHAPTER TWO

DESIGN AND ANALYSIS OF ROTMAN LENS

Design of Rotman lens [2, 3] involves both geometric trade and mutual coupling effects between the lens ports. The shape of lens determines the mutual coupling between the ports. It is difficult to control the mutual coupling. Thus a careful geometric optics design should be accomplished first and then parameters should be optimized to obtain the desired response. This chapter describes design of Rotman lens using ray optics approach and effects of design parameters on the shape of the lens and on the path length error. The designed lens has been analyzed using two-dimensional field analysis approach. The term "analysis" denotes the determination of the circuit parameters for its multi port model. Results obtained have been compared with the results predicted by its design approach.

2.1 DESIGN PROCEDURE

Figure 2.1 shows the cross- section of a trifocal Rotman-type lens. One focal point F_0 is located on the central axis and the two others F_1 and F_2 are symmetrically located on either side on a circular focal arc (also called feed contour). Contour I_2 is a straight line and defines the position of the radiating elements. I_1 is the inner contour of the lens (also called the array contour). Two off axis focal points F_1 and F_2 are located on the focal arc at angles $+\beta$ and $-\beta$. It is required that the lens be designed in such a way that outgoing beams make angles $-\alpha$, 0 and $+\alpha$ with the x axis when feeds is placed at F_1, F_0 and F_2 respectively. Rotman lens has the following four design parameters:

1. Off axis focal length F: This is the distance between off axis focal point and mid point of the array contour (distance O_1F_1 or O_1F_2 as defined in Figure 2.1)
2. On axis focal length G: This is the distance between on axis focal length and mid point of the array contour (distance O_1G as defined in figure 2.1).

3. Antenna element spacing d: Radiating elements are located along the straight line I_2. Number of antenna elements and spacing between antenna elements determines the length of contour I_2 (this is also called lens aperture).

4. Scanning angle α: Scanning angle determines the angular coverage provided by the lens. The lens can cover an angular area $\pm \alpha$.

It may be noted that in this proposed approach the two off axis focal points are located at angles $\pm \beta$ whereas in the approach suggested in [2] these were located at angles $\pm \alpha$. Using the design approach suggested in [2] following equations are written

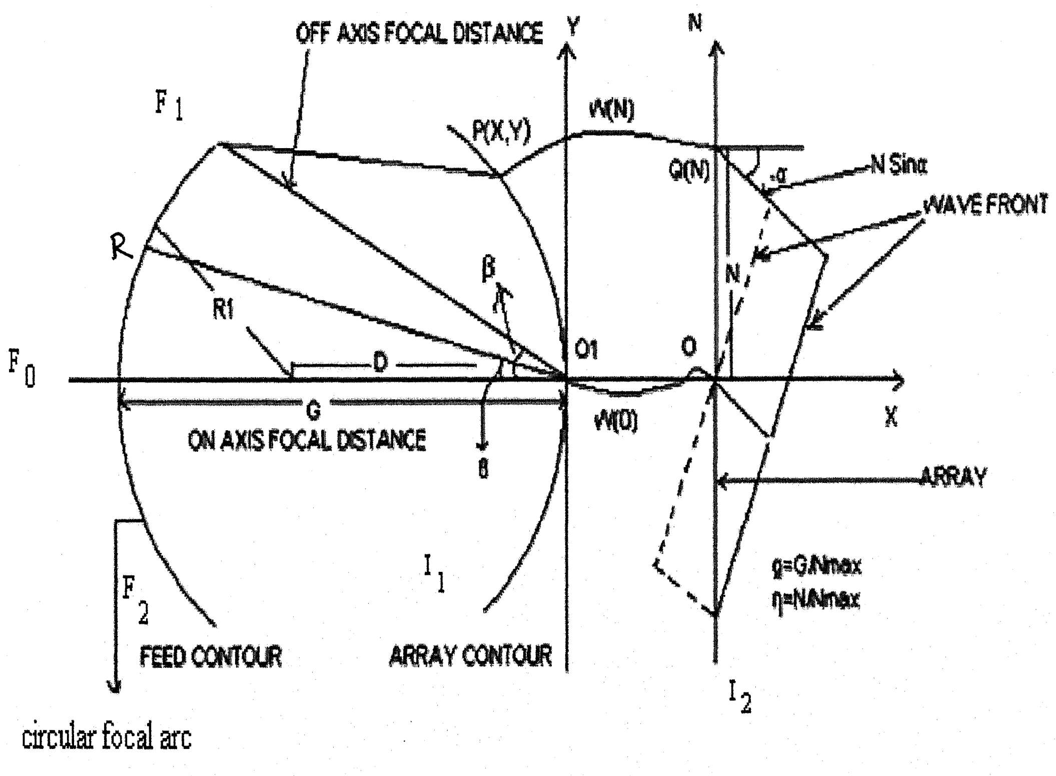

FIGURE 2.1 CROSS SECTION OF TRIFOCAL ROTMAN LENS

$$\sqrt{\varepsilon_r}\,(F_1P)+\sqrt{\varepsilon_{re}}\,W(N)+N\sin\alpha=\sqrt{\varepsilon_r}\,F+\sqrt{\varepsilon_{re}}\,W(O) \tag{2.1}$$

$$\sqrt{\varepsilon_r}\,(F_2P)+\sqrt{\varepsilon_{re}}\,W(N)-N\sin\alpha=\sqrt{\varepsilon_r}\,F+\sqrt{\varepsilon_{re}}\,W(O) \tag{2.2}$$

$$\sqrt{\varepsilon_r}\,(F_0P)+\sqrt{\varepsilon_{re}}\,W(N)=\sqrt{\varepsilon_r}\,G+\sqrt{\varepsilon_{re}}\,W(O) \tag{2.3}$$

Where

$$(F_1P)^2=(X+F\cos\beta)^2+(Y-F\sin\beta)^2 \tag{2.4}$$

$$(F_2P)^2=(X+F\cos\beta)^2+(Y+F\sin\beta)^2 \tag{2.5}$$

$$(F_0P)^2=(X+G)^2+(Y)^2 \tag{2.6}$$

$N =$ Indicate the position of the radiating elements, called the lens aperture.

ε_r = Substrate dielectric constant.

ε_{re} = Effective dielectric constant of the transmission lines.

Design parameters are normalized relative to the maximum lens aperture N_{max} and defined as follows

$f = F / N_{max}$

$g = G/N_{max}$

$w = (W(0) - W(N))\sqrt{\varepsilon_{re}}/(\sqrt{\varepsilon_r}\,N_{max})$

$\eta = N/N_{max}$

$y = Y/N_{max}$ and

$x = X/N_{max}$

Algebraic manipulation of the above equations gives

$$y=\eta\sin\alpha\,(f+w)/\sqrt{\varepsilon_r}\,f\sin\beta \tag{2.7}$$

$$x=a+b\,w \tag{2.8}$$

$$A\,w^2+B\,w+C=0 \tag{2.9}$$

Where

$a = (\eta\sin\alpha)^2/(2\varepsilon_r\,(f\cos\beta - g))$

$b = (f - g)/(f\cos\beta - g)$

$A = b^2 + \eta^2 \sin^2\alpha/(\varepsilon_r f^2 \sin^2\beta) - 1$

$B = 2ab + 2(\eta^2\sin^2\alpha/\varepsilon_r f\sin^2\beta) + 2gb - 2g$

$C = a^2 + \eta^2(\sin^2\alpha/\varepsilon_r \sin^2\beta) + 2ga$

For the given value of design parameters F, G, N_{max} and α it is required to calculate the value of β, such that the height of the two contours (feed and array contour) be equal. Y- Coordinate of array contour is given by equation (2.7). For maximum value of lens aperture i.e

$N = N_{max},\quad \eta=1$ and

$$y_{max} = \sin\alpha\,(f + w)/(\sqrt{\varepsilon_r}\, f\sin\beta) \qquad (2.10)$$

To equalize the height of the two contours Y coordinate of the feed contour i.e $f\sin\beta$ must be equal to y_{max} i.e.

$$f\sin\beta = \sin\alpha\,(f + w)/(\sqrt{\varepsilon_r}\, f\sin\beta) \qquad (2.11)$$

Using equations (2.7), (2.8), (2.9), and (2.11) value of β can be calculated for given value of α, F, G, N_{max} and ε_r. The lens designed using the calculated value of β will have equal height of the feed and array contour.

Figure 2.1 (a) shown the variation of β with α. As the value of α increases, the value of β also increases. Figure 2.1(b) shown the variation of β with f. As the value of f increase the value of β decreases. Figure 2.1(c) shown the variation of β with N_{max}. As value of N_{max} increases the value of β also increases.

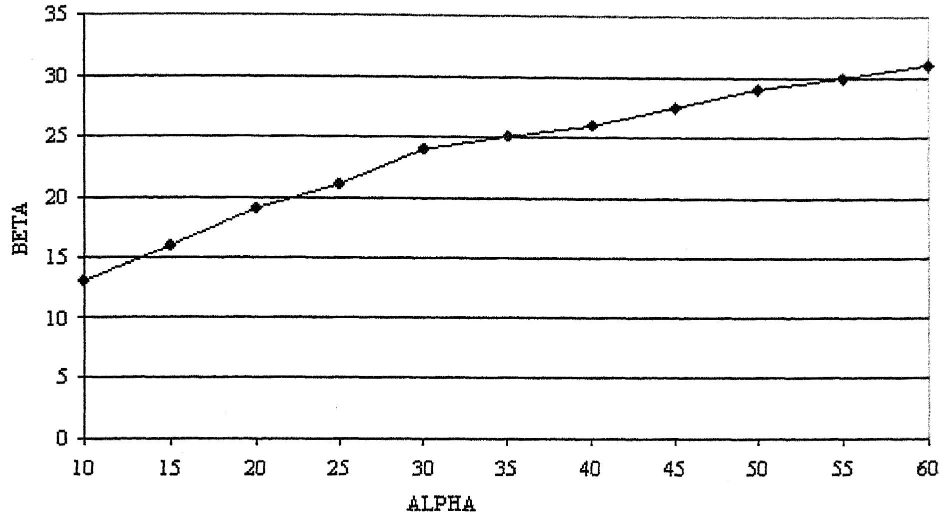

(f=1.70, g=1.74, ε_r=3.7, N_{max}=5.4in., Frequency=3.4641GHz)

FIGURE 2.1(a):VARIATION OF BETA WITH ALPHA

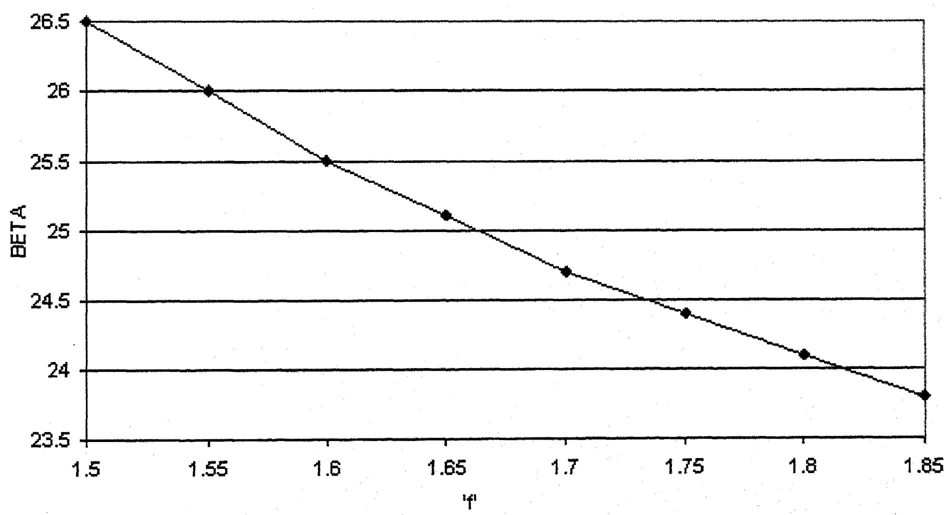

(g=1.74,ά=35deg., ε_r=3.7,N_{max}=5.4in.,Frequency=3.4641GHz)

FIGURE 2.1(b): VARIATION OF BETA WITH 'f'

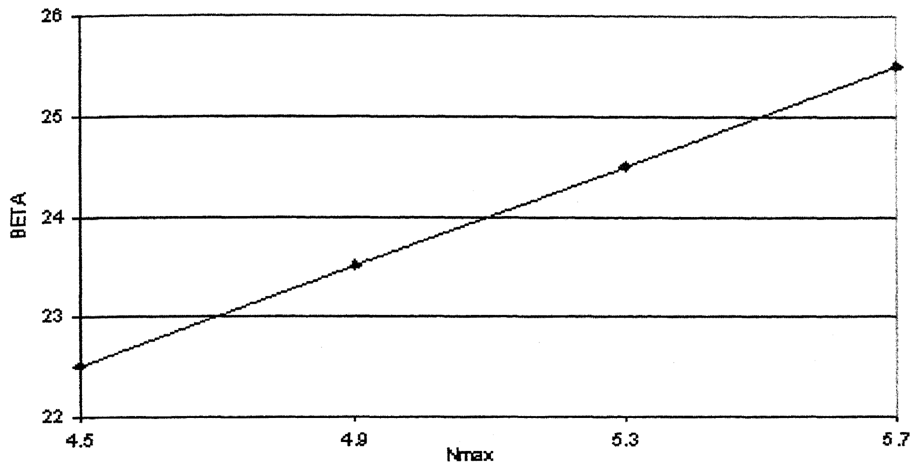

(f=1.70,g=1.74,α=35,ε =3.7,Frequency=3.4641 GHz)

FIGURE 2.1(c): VARIATION OF BETA WITH Nmax

2.2 EFFECTS OF DESIGN PARAMETERS ON THE SHAPE OF THE LENS.

Rotman lens has four basic design parameters, focal angle α, off axis focal length F, on axis focal length/N_{max} and lens aperture η. For any lens design usually scanning angle and number of antenna elements are specified. Then it is required to select the proper value of the design parameters. Path length error and lens shape depend upon these parameters. Lens shape determines the mutual coupling between port, multiple scattering between the ports and spillover losses.

Shape of the lens is important factor, which determines the power coupling from the feed contour to the array contour. This section describes the dependence of the shape of the lens on the design parameters.

Figure 2.2(a) shown the effect of 'f' on the shape of the lens. It is shown that as 'f' increase, the feed contour open and array contour closes.

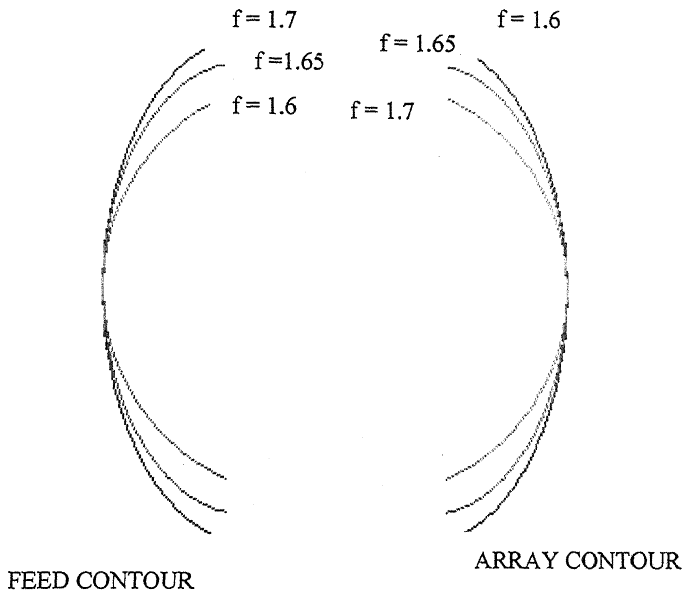

FIGURE 2.2(a) EFFECT OF " f " ON THE SHAPE OF THE LENS

Figure 2.2(b) shown the effect of focal angle α on the shape of the lens. As the value of α increases, the array contour closes and feed contour opens. The value of α is selected in such a way the height of both the contours are almost equal. The value of α also increase the path length error and therefore this factor must be considered in designing optimum shape of the lens

The height of the array contour is a function of the lens aperture (η). As η increases, the height of the array contour increases. The lens aperture also determines the spacing between the array elements. Element spacing is a critical parameter since it controls the appearance of grating lobes. For maximum scanning angle θ_{max} ,the spacing d that just admit a grating lobe is given by[21]

$$d/\lambda = 1/(2+\sin\theta_{max}) \qquad (2.12)$$

where d is the antenna element spacing and λ is the wavelength.

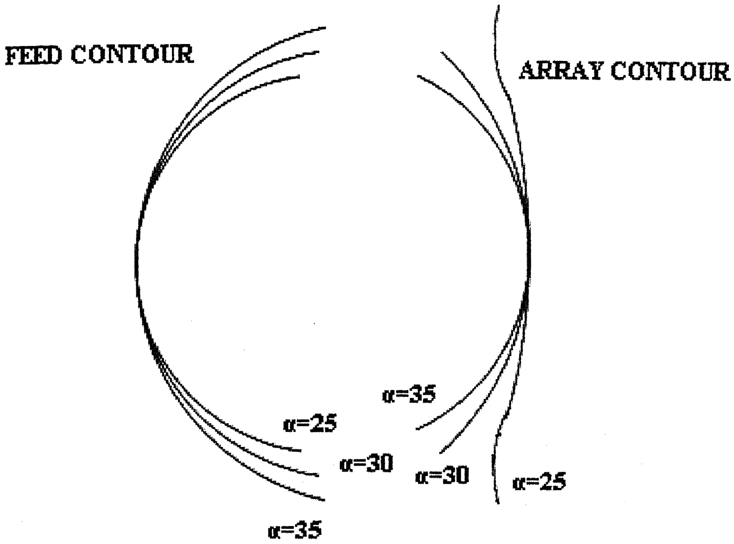

FIGURE 2.2(b) EFFECT OF FOCAL ANGLE(α) ON THE GEOMETRY OF THE LENS

In general antenna element spacing is kept below this value. Hence, α and η should be selected in such a way that the height of both the contours are almost equal. Equal height of both the contour is required to couple maximum power from the feed contour to array elements.

The dependence of the lens contour on "g" is shown in figure 2.3. As "g" increases, the array contour opens and the feed contour closes. It may be noted that increasing 'g' has reverse effect to that with the increase in α. In Rotman lens feed contours and array contours are open boundaries, they never meet and it is required to cover this gap by microwave absorbers. As the value of "g" increases, the gap between feed contour and array contour increases. So small value of "g" gives a compact lens. A compact lens has less spillover losses.

Off axis focal length F has no effect on the shape of the lens it only change the dimensions of the lens.

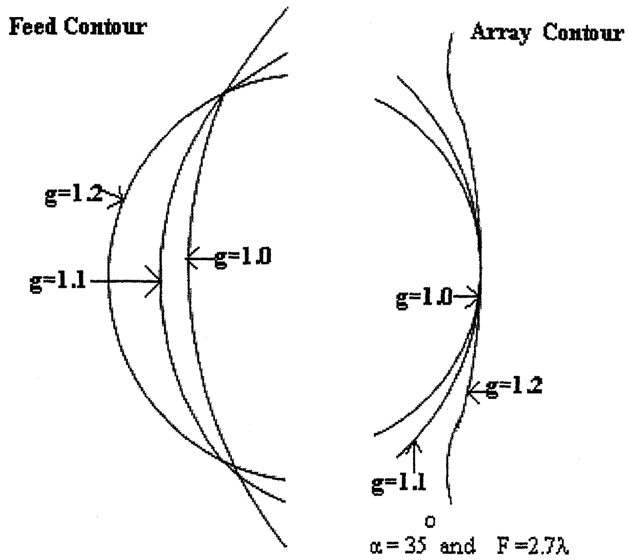

FIGURE 2.3 EFFECTS OF 'G' ON GEOMETRY OF LENS

2.3 PHASE ERROR

Path length error for the lens is defined as [2] the difference in path length between a central ray through the origin and any other ray, both of which are traced from an arbitrary point on the focal arc through the lens and terminates normal to the emitted wave front.

When a feed is placed at one of the focal point, corresponding emitted wave front has no phase error. When the feed is displaced from the focal point, the corresponding wave front will have a phase error. However for wide angle scanning lens must be focused at all the intermediate points along the focal arc. Let a feed be located at point R (Figure 2.1) on the focal arc for the out going beam at an angle θ. Let R_a and R_b be the phase shift from the feed position to the wave front when the ray is passing through P (X,Y) and O respectively. The phase error is given by

$$\delta L = R_a - R_b \tag{2.12}$$

Where

$$R_a = \sqrt{\varepsilon_r}\,(RP) + \sqrt{\varepsilon_{re}}\,W\,(N) + N \sin\theta$$

$R_b = \sqrt{\varepsilon_r}\ (RO) + \sqrt{\varepsilon_{re}}\ W(O)$

Figure 2.4 shows the variation of the normalized phase error ($\delta L/N_{max}$) with the normalized lens aperture for different value of scanning angles (θ).When the phase angle (θ) is equal to 20° the normalized phase error is minimum. As theta increases the normalized phase error increases.

Figure 2.5 shows the variation of normalized phase error with normalized lens aperture for different values of lens aperture N_{max}. Phase error increases as the lens aperture increases.

Figure 2.6 shows the variation of normalized phase error with "f" for different values of scanning angles. It may be noted that error is minimum at specific value of "f". The normalized phase error is neither minimum at very small values nor at very large values, it is minimum at some intermediate values.

Figure 2.7 shows the variation of normalized phase error with "g" for different values of scanning angles. It may be noted that error is minimum at a specific value of "g". The normalized phase error is neither minimum at very small values nor at very large values, it is minimum at some intermediate values.

Figure 2.8 shows the variation of normalized phase error "α" for different scanning angles. Phase error is 0 for $\alpha = \theta$.

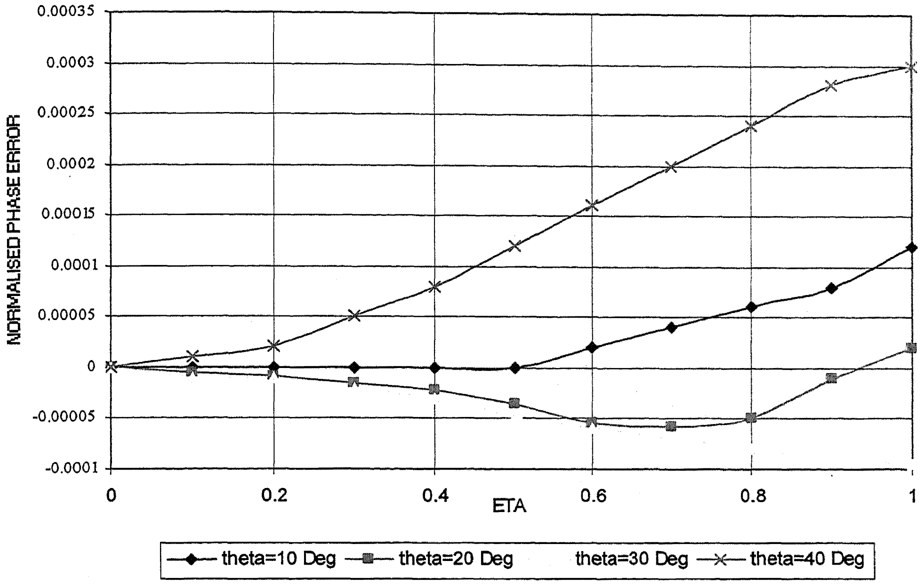

FIGURE2.4 NORMALISED PHASE ERROR VERSUS ETA

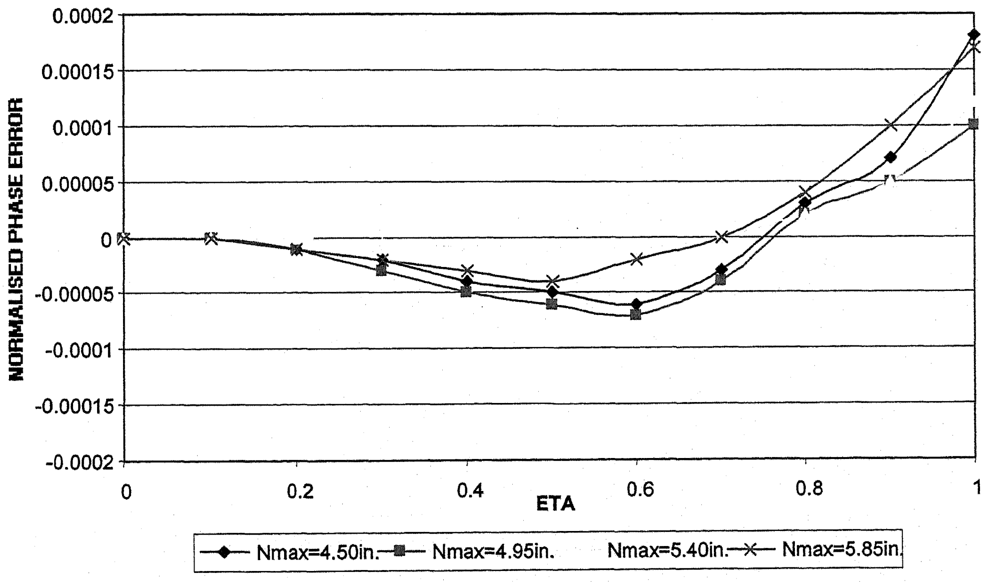

FIGURE 2.5 NORMALISED PHASE ERROR VARIATION WITH Nmax

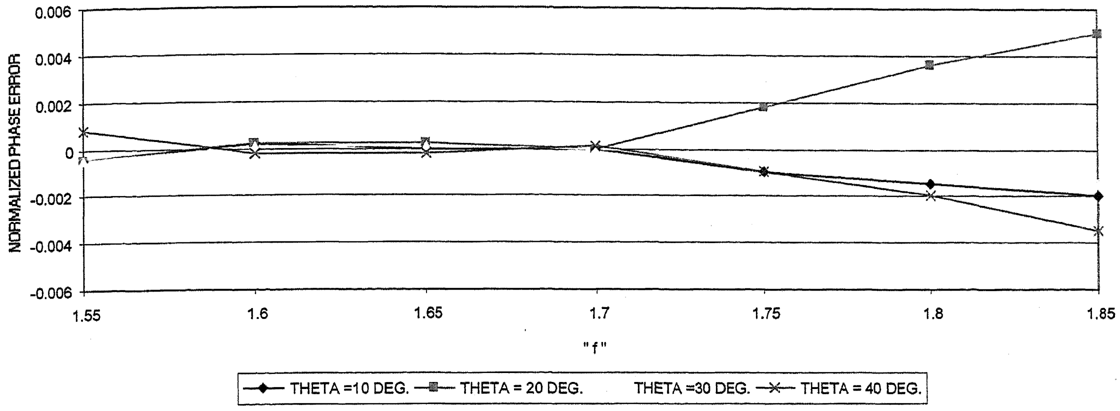

FIGURE.2.6 NORMALIZED PHASE ERROR VERSUS "f"

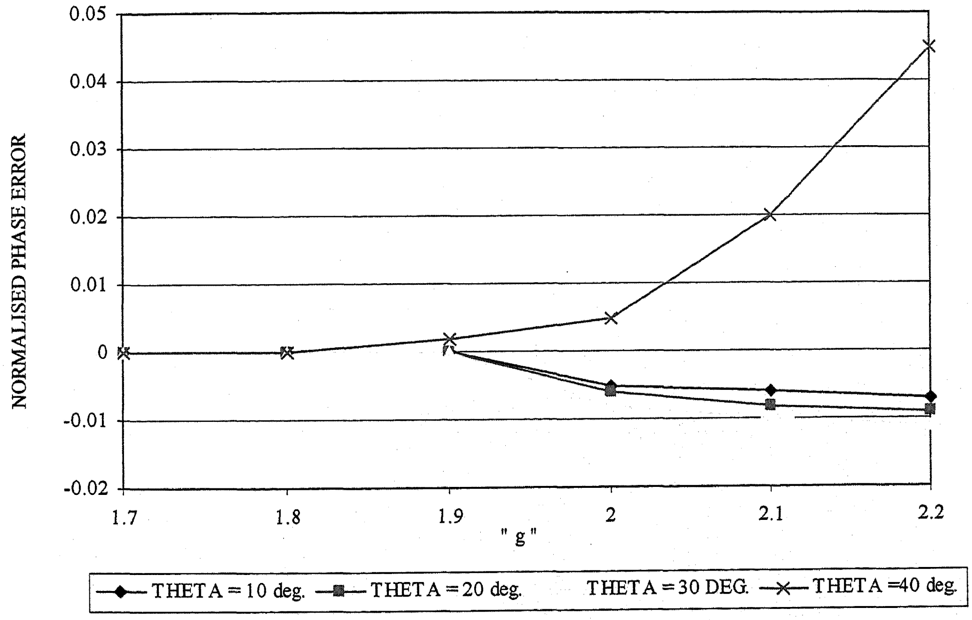

FIGURE 2.7 NORMALISED PHASE ERROR VERSUS " g "

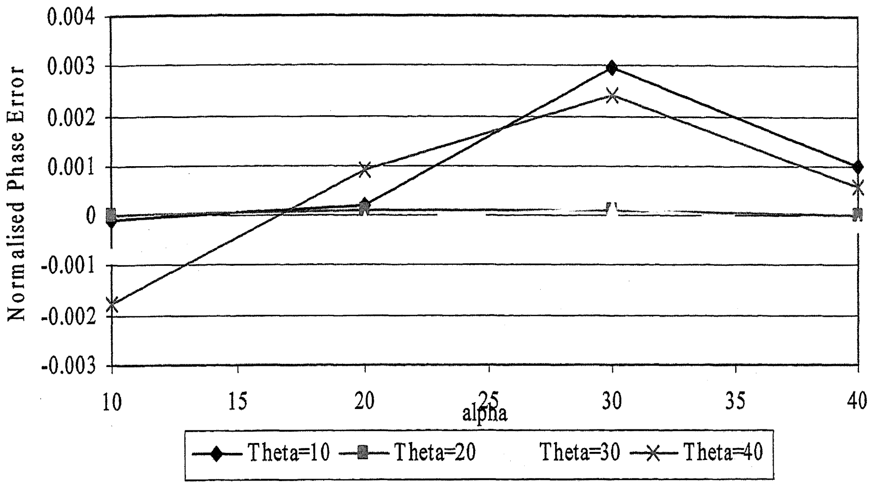

FIGURRE 2.8:NORMALISED PHASE ERROR VERSUS ALPHA

2.4 TWO-DIMENSIONAL FIELD ANALYSIS OF THE LENS

In microstrip or stripline configuration of the lens, the height (thickness) is much smaller than the wavelength at the operating frequencies and consequently, there is no variation of the fields along the height of the substrate. To analyze such a planar circuit out of several methods [42,52] developed so far, contour integration method [42] is most suitable, because of the arbitrary geometrical shape of the lens.

2.4.1 FORMULATION OF CONTOUR INTEGRAL METHOD

Consider an arbitrary planar circuit in microstrip configuration, having several ports as shown in figure 2.9. Using Weber's solution for cylindrical waves, the potential V (s) at a point upon the periphery of the circuit geometry is found to satisfy the following integral equations [52].

$$V(s) = (1/2j)\int_c \{k\cos\theta H_1^{(2)}(kr)V(s_0) - j\omega\mu H_0^{(2)}(kr)i_n(s_0)\}ds_0 \qquad (2.15)$$

Where $H_0^{(2)}$ and $H_1^{(2)}$ are the zero order and first order Hankel functions of the second kind respectively, i_n denote the current density flowing outwards along the

periphery. The variable r denotes distance between points M and L on the periphery, d is the substrate thickness and s and s_0 are the location of the field and source points respectively along the periphery. The angle between the line joining the points M and L and the normal at point L is denoted by θ. ω, k and μ are the angular frequency, wave number and permeability of the spacing material respectively. Equation (2.15) is a contour integral over the periphery of the planar circuit and is the reason for the name of this method. A detailed derivation of this integral expression is given in [42, 52].

Equation (2.15) gives the relation between the R.f. Voltage and R.f. Current distributed along the periphery. To solve the equation (2.15) numerically the circuit

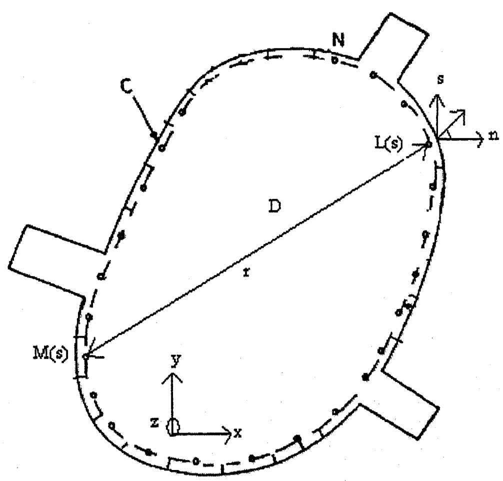

FIGURE 2.9: ARBITRARY SHAPED PLANAR CIRCUIT

periphery is divided into N incremental sections numbered as 1,2,3...N having widths W_1, W_2, W_3,........W_N respectively as shown in figure 2.10. Coupling ports are assumed to occupy each one of those sections. When width of various sections is small, field intensity may be assumed uniform over each section (port width) and equation (2.15) yield a system of matrix equation [42].

$$\sum_{j=1}^{n} u_{ij} v_j = \sum_{j=1}^{n} h_{ij} I_j \qquad (I = 1, 2, 3....N) \qquad (2.16)$$

Where

$$u_{ij} = \delta_{ij} - (k/2j)\int_{wj} \cos\theta H_1^{(2)}(kr)ds \qquad (2.17)$$

And

$$h_{ij} = (\omega\mu d/4wj)\int_{wj} H_0^{(2)}(kr)ds \qquad \text{(For } i \neq j\text{)}$$

$$= (\omega\mu d/4)[1-(2j/\pi)(InkW_i/4-1+\gamma)] \qquad \text{(For } i = j\text{)} \qquad (2.18)$$

$\gamma = 0.5772\ldots$ is Euler's constant and $\delta_{ij}= 1$(for i = j) and zero otherwise. Solving equation (2.16) one obtains the R.F. voltage on each sampling point as

$$V = U^{-1}\ HI \qquad (2.19)$$

Where V and I denote column vectors consisting of Vi and I_i and U and H are NXN matrices consisting of U_{ij} and H_{ij} respectively. The matrix U^{-1} is the inverse of matrix U.Z matrix for the N port network of figure 2.10 is given by

$$Z= U^{-1}\ H \qquad (2.20)$$

2.4.2 NUMERICAL COMPUTATION

For numerical computation of the Z –matrix of the multi port network discussed in previous section, divide the periphery of the circuit into N sections and approximate these sections by straight-line elements (figure 2.10). These dividing points are numbered i =1, 2 ,3…N in the counter clockwise direction and their coordinates are denoted as (X (i), Y(i)). The sections between the i^{th} and $(i+1)^{th}$ dividing points are called i^{th} section and sampling points are set at the centre of each section, so that its coordinates (SX(i),SY(i)) are given as

$$SX(i) = (X(i) + X(i+1))/2 \qquad (2.21)$$

$$SY(i) = (Y(i) + Y(i+1))/2 \qquad (i = 1, 2, 3\ldots N) \qquad (2.22)$$

And the width of i^{th} section is given as

$$W_i = \sqrt{(X(i+1)-X(i))^2+(Y(i+1)-Y(i))^2} \qquad (2.23)$$

The width of the sections need not be equal to each other usually it is desired to use narrower sections at positions where the curvature is large, because the circuit periphery is approximated by a piece wise linear pattern.

The distance r_{ij} between the i^{th} and j^{th} sampling point is given by

$$\sqrt{\{SX(i)-SX(j)\}^2+\{SY(i)-SY(j)\}^2} \qquad (2.24)$$

Let the angle made by the line connecting the points i^{th} and j^{th} and the normal at the i^{th} sampling point be devoted by θ_{ij} if θ_j denotes the angle between X – axis and the line having the direction from point [X (j), Y (j)] to point [X (j +1), Y (j + 1)], one can write as

$$\cos\theta_{ij} = [\{ SX(j) - SX(i) \}\sin\theta_j - \{SY(j) - SY(i)\}\cos\theta_j] / r_{ij} \qquad (2.25)$$

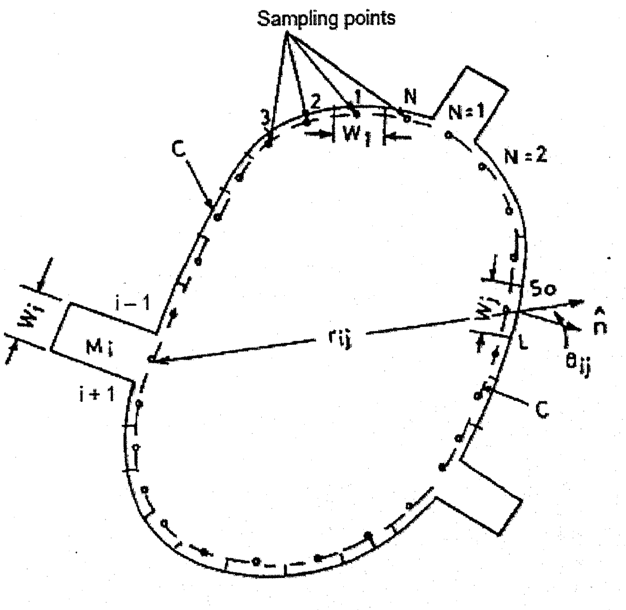

FIGURE 2.10: GEOMETRY SHOWING THE SYMBOL USED IN THE NUMERICAL ANALYSIS

By using the relation

$$\cos\theta_j = \{ X(j + 1) - X(j) \}/ W_j \qquad (2.26)$$

$$\sin\theta_j = \{ Y(j+1) - Y(j) \}/ W_j \tag{2.27}$$

Equation 2.25 can be written as

$$\cos\theta_{ij}=\{[SX(j)-SX(i)][Y(j+1)-Y(j)]-[SY(j)-SY(i)][X(j+1)-X(j)]\}/r_{ij}Wj \quad \text{For } i \neq j \tag{2.28}$$

$$= 0 \quad \text{for } i = j$$

Thus θ_{ij} can be computed from the coordinates of sampling and dividing points. The matrix elements u_{ij} and h_{ij} as discussed earlier can be calculated by computing the integrals using Simpson's method. However these can be computed approximately, without computation of integrals as

$$u_{ij} = \delta_{ij} -(k/2j)\cos\theta_{ij} H_1^{(2)} (k\, r_{ij})\, W_j \tag{2.29}$$

and

$$h_{ij} =(\omega\mu\, d/4)\, H_0^{(2)} (k\, r_{ij}) \tag{2.30}$$

The choice between the above two alternative approaches depends upon accuracy required and computation time.

2.5 GUIDELINES TO SELECT THE DESIGN PARAMETERS

Considering the effects of design parameters on the shape of the lens and on the phase error following guidelines to selects the design parameters are recommended.

1. Select α = specified scanning angle.
2. Lens aperture N_{max} is a function of antenna element spacing. Antenna element spacing controls the appearance of grating lobes [21]. To control the grating lobe it is required that the antenna element spacing

$$D < \lambda / (2 + \sin\psi_m) \tag{2.31}$$

Where ψ_m is the maximum scanning angle and λ is the wavelength. For $\psi_m = \alpha$ antenna element spacing and then N_{max} can be calculated. Considering the dependency of phase error and shape of the lens on "f" and "g", suitable values of "f" and "g" may be selected.

2.5.1 ANALYSIS

In the microstrip or stripline configuration, the thickness of the lens substrate is much smaller than the wavelength at the operating frequencies, and consequently there is no variation of the field along the height of the substrate. This type of planar circuit may be considered a two-dimensional circuit. Because of the arbitrary geometrical shape of the lens, the contour integral method [36] has been adopted to analyze the proposed lens geometry. More detail of the contour integral technique has been given in [36, 42].

To analyze the lens using the contour integral approach, the array contour divided in to 12 ports as shown in figure 2.11. Out of the 12 ports, 10 ports used as array ports and two are used as dummy ports. Similarly, the feed contour is divided into 11 ports, two ports being dummy ports and nine feed ports. Therefore the lens has total of 23 ports. Each of the dummy ports is terminated into a 50-ohms dummy load. The input and the output ports are connected to the source and the antenna elements respectively through a 50-ohms transmission lines and taper section. The port number notation used in the analysis is shown is figure 2.11.

2.5.2 SPECIFIC DESIGN EXAMPLE

This section describes a theoretical example of the design and analysis of the Rotman-type lenses to feed array of wave-guide horns, with the following requirements:

Angular coverage = $\pm 35^0$

Number of antennae elements =10

Number of input beam = 09

Central frequency = 3.4641 MHz

The complete structure is assumed to be fabricated in microstrip version on substrate of thickness 1/16 inch and dielectric constant 3.7.The loss tangent is 0.001.

Two lenses have been designed for the above requirement. As per the guidelines recommended earlier following design parameters have been selected for the two lenses.

1. Lens 1; $\alpha = 35^0$, $f = 1.70$, $g = 1.74$

Spacing between antenna elements =1.2 inch

2. Lens 2 ; $\alpha = 35^{0,}$ $f = 1.70$, $g = 1.86$

Spacing between antenna elements = 1.2 inch

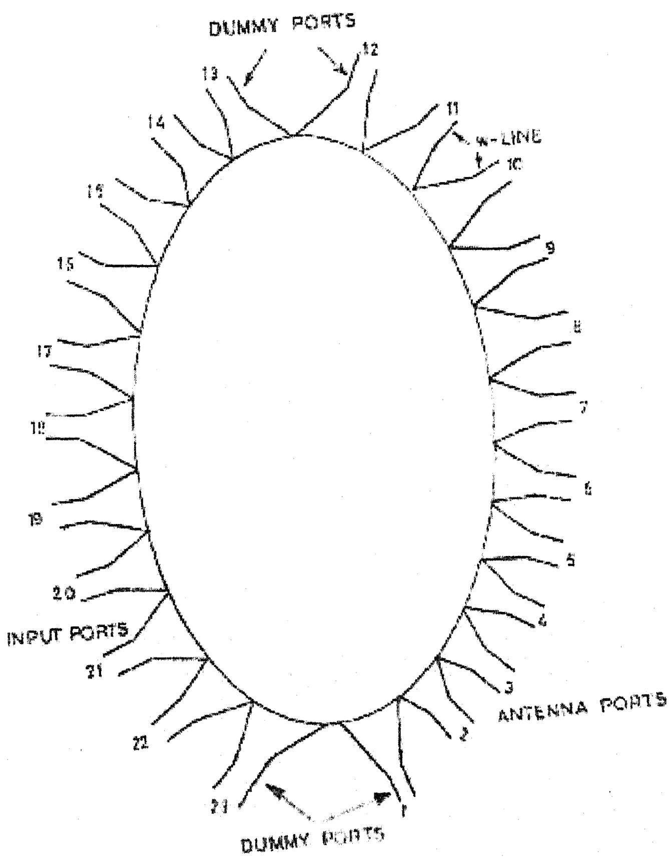

FIGURE 2.11: LENS IN ITS MULTI PORT GEOMETRY

2.5.3 RESULTS AND DISCUSSION

Figure 2.12 shows the design lens contour with beam port on the left and element port on the right. For different value of "g" array contour are shown. It is clear from the figure by increasing the value of "g" the array contour increase.

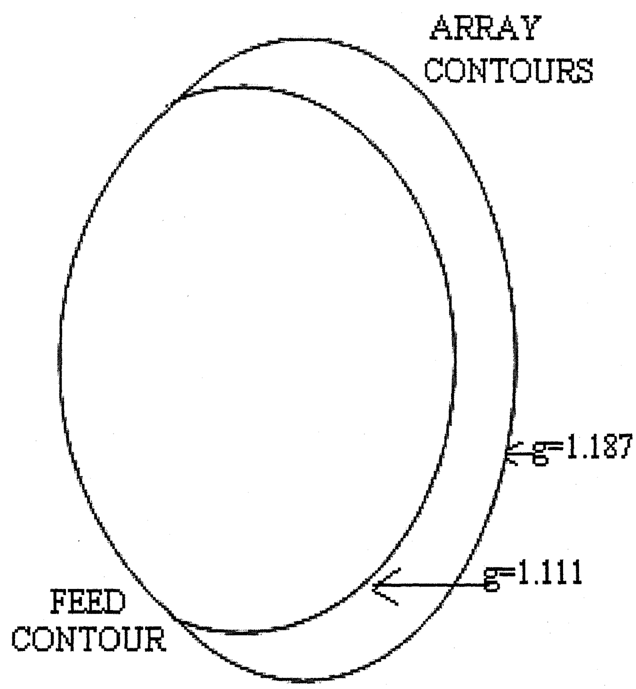

FIGURE 2.12: DESIGNED LENS CONTOURS

Figure 2.13 shows the reflection coefficient at the input port in view of the geometrical symmetry, reflection coefficient for only five input ports are shown (the ports are numbered as shown in figure 2.11). The variation of reflection coefficient for lens 1 is – 22.47 dB to – 8.64 dB and the variation of reflection coefficient for lens 2 is -12.34 dB to – 10.52 dB.

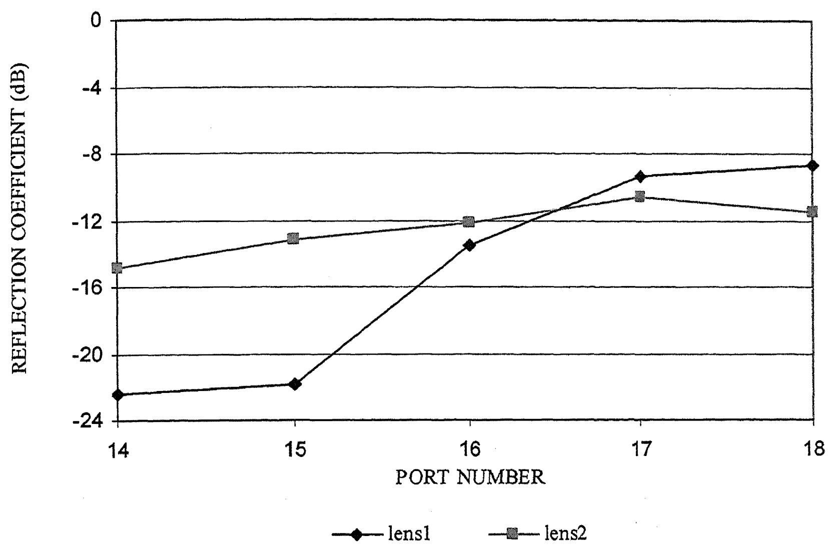

FIGURE 2.13 REFLECTION COEFF. AT INPUT PORTS FOR ROTMAN LENS

Amplitude distribution across the array ports for both the lenses are shown in figure (2.14a – 2.14e). When input applies at port number 14 the coupling coefficient is minimum at port number 10 for lens 1 and at port number 6 for lens 2. When input applies at port number 15 the coupling coefficient is minimum at port 5 for lens 1 and at port 7 for lens 2. When input applies at port number 16 the coupling coefficients is minimum at port 8 for lens 1 and 2. When input applies at port number 17 the coupling coefficient is minimum at port 6 for lens 1 and 2. When input applies at port number 18 the coupling coefficient is minimum at port 4 and 9 for lens 1 and port 7 for lens 2.

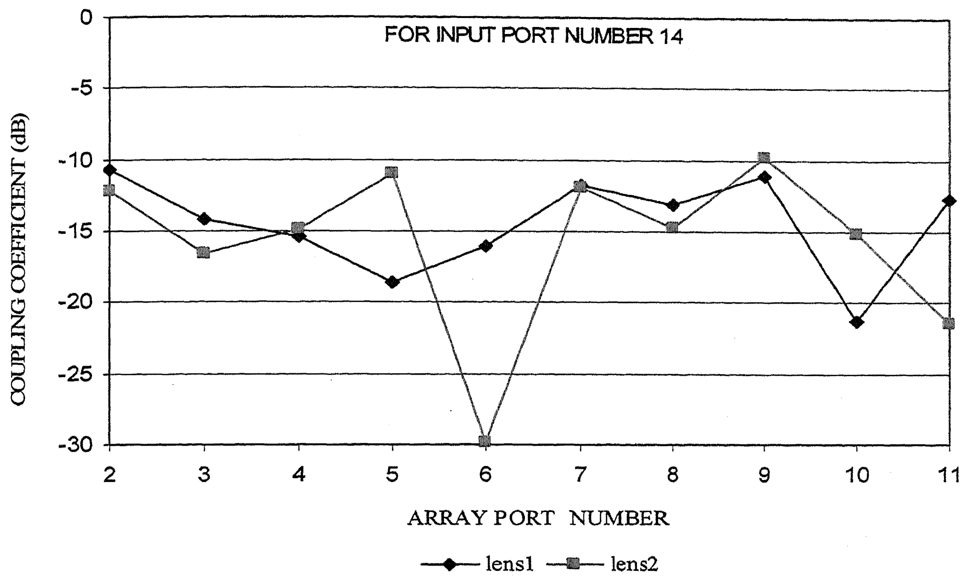

FIGURE 2.14(a) AMPLITUDE DISTRIBUTION ACROSS ARRAY PORT

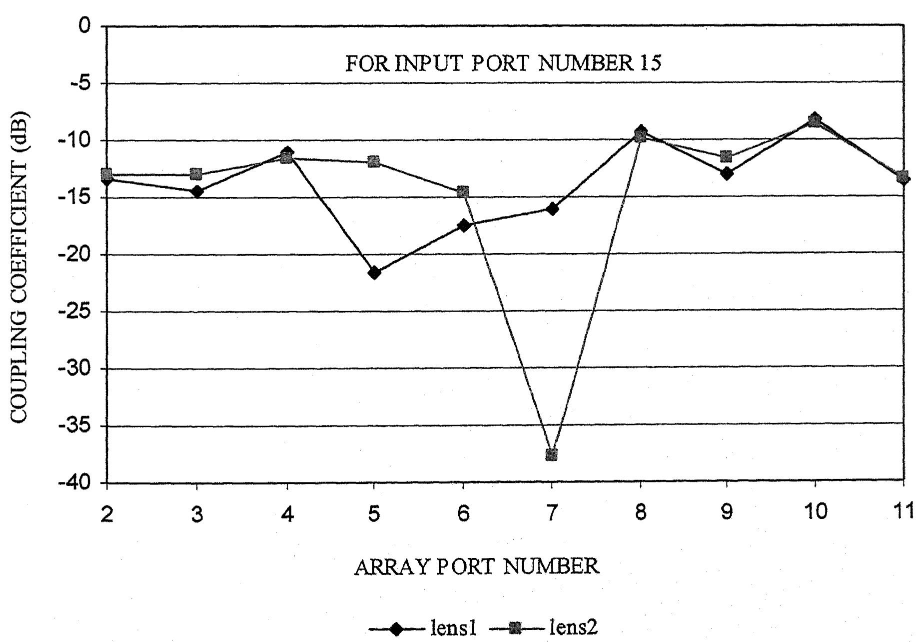

FIGURE 2.14(b) AMPLITUDE DISTRIBUTION ACROSS ARRAY PORT

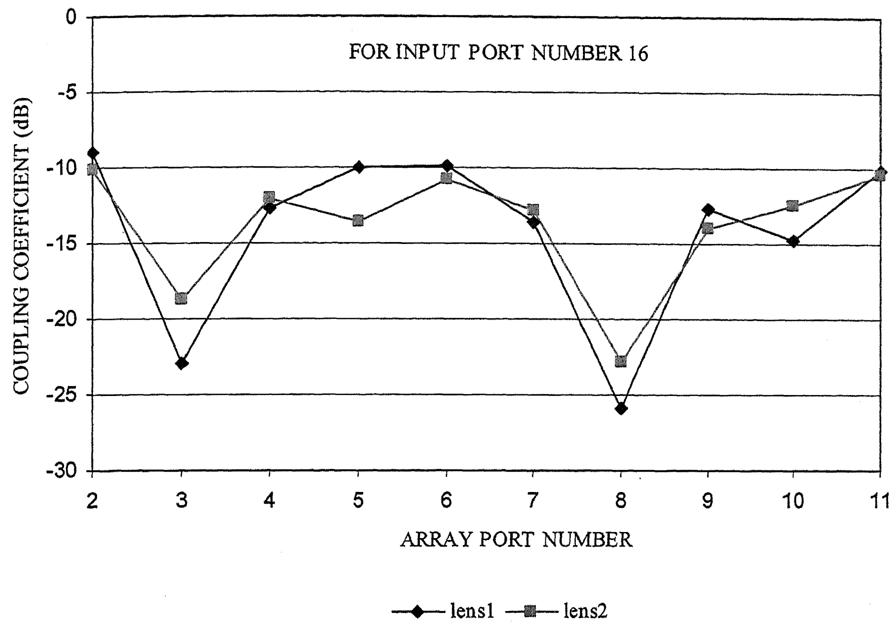

FIGURE 2.14(c) AMPLITUDE DISTRIBUTION ACROSS ARRAY PORT

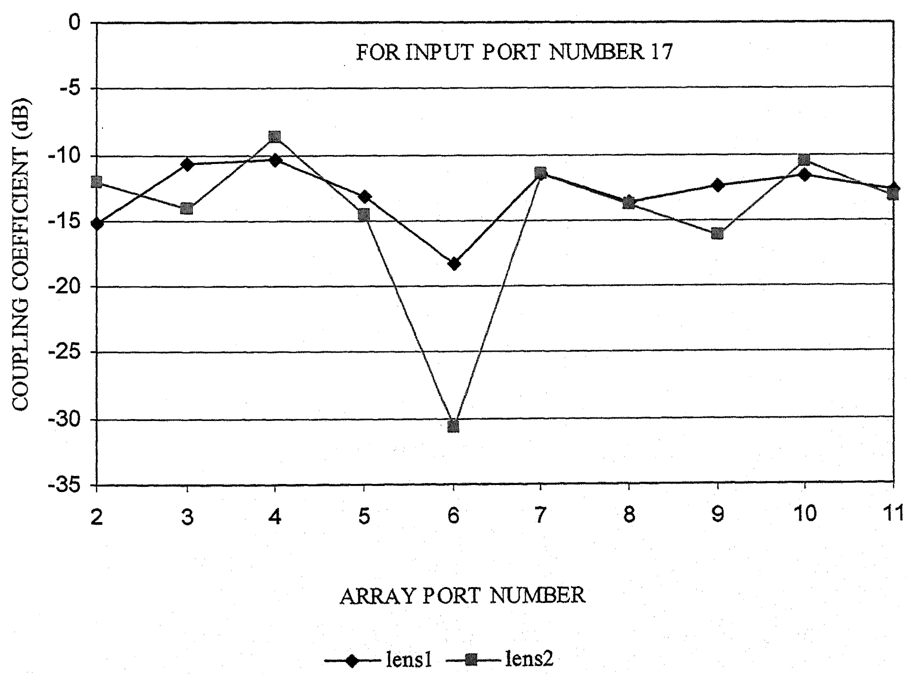

FIGURE 2.14(d) AMLITUDE DISTRIBUTION ACROSS ARRAY PORT

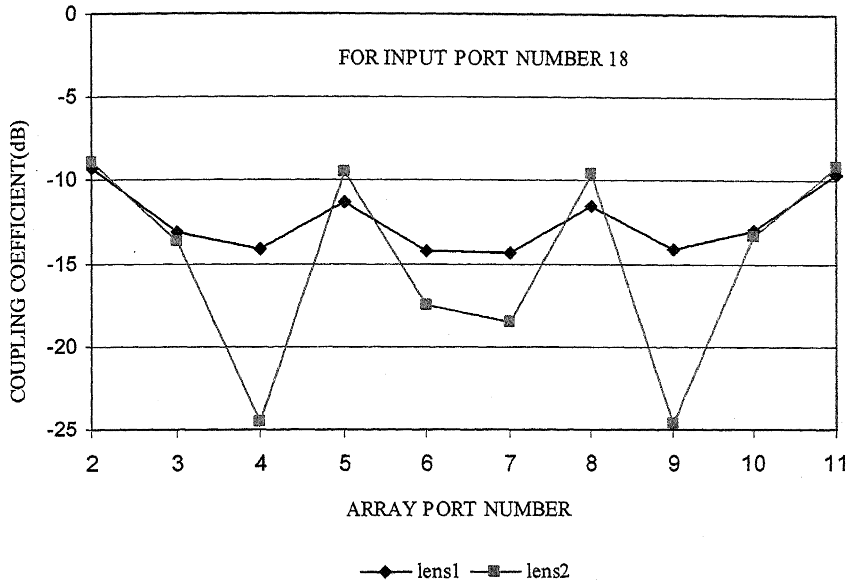

FIGURE 2.14(e) AMPLITUDE DISTRIBUTION ACROSS ARRAY PORT

Phase distribution across the array ports for both the lenses is shown in figure (2.15a – 2.15e). For input port number 14, 15 and 17 the phase distribution across the array port for lens 1 and lens 2 are almost equal. For input port number 16 and 18 the phase variation across the array port is approximate two radians.

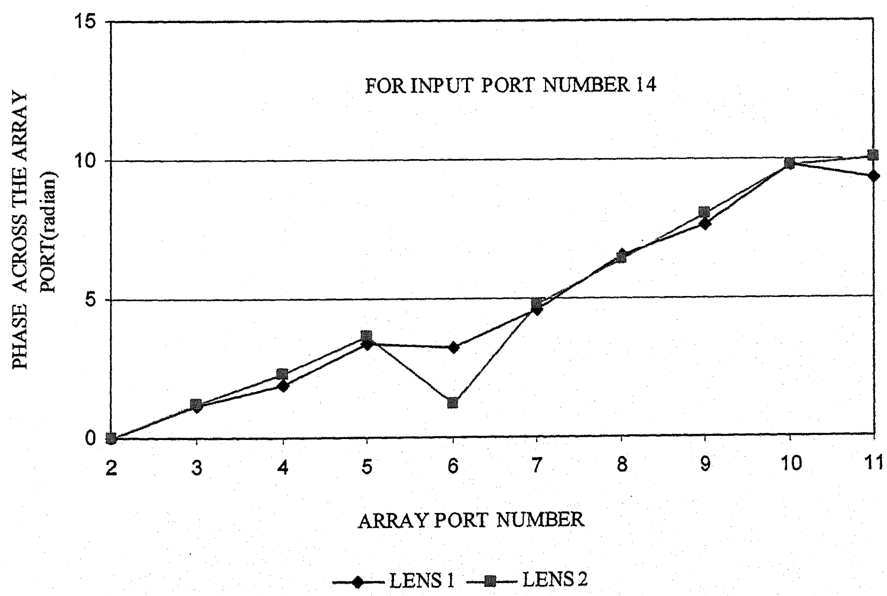

FIGURE 2.15(a) PHASE DISTRIBUTION ACROSS THE ARRAY PORT

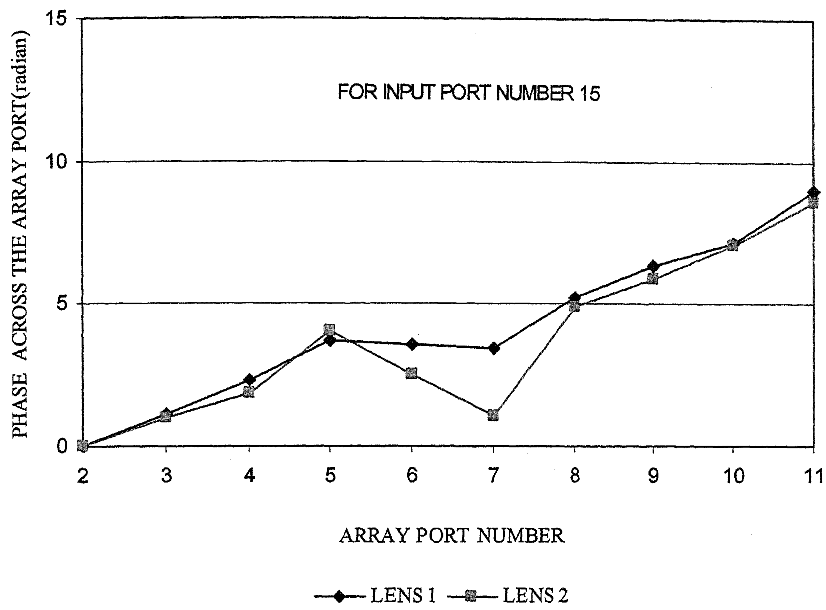

FIGURE 2.15(b) PHASE DISTRIBUTION ACROSS THE ARRAY PORT

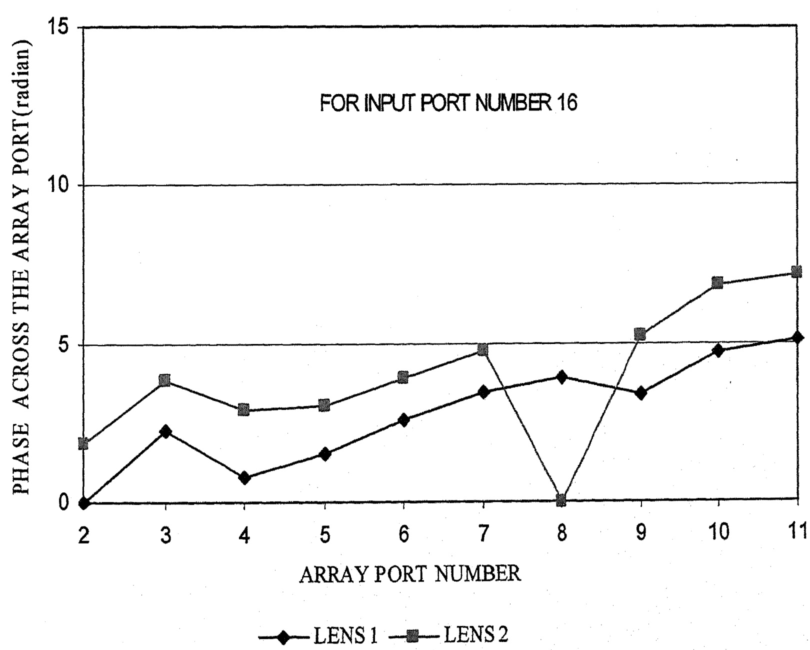

FIGURE 2.15(c) PHASE DISTRIBUTION ACROSS THE ARRAY PORT

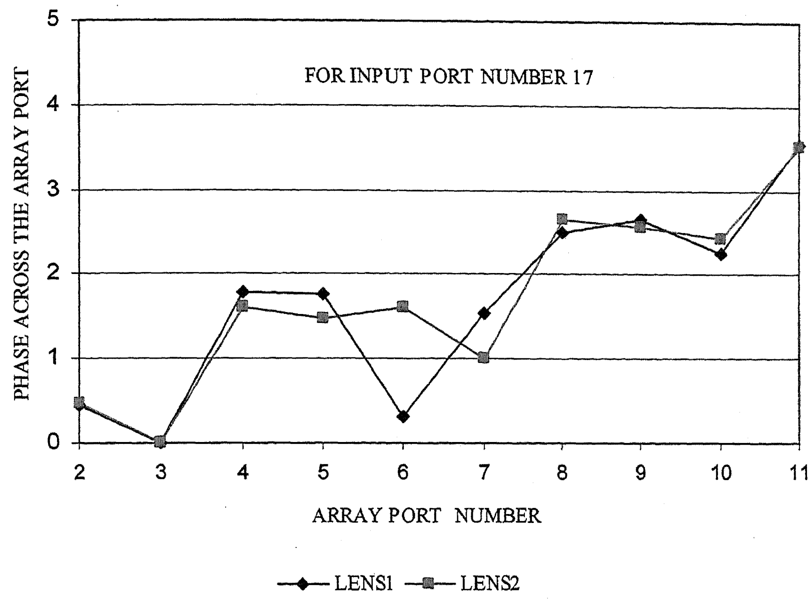

FIGURE 2.15(d) PHASE DISTRIBUTION ACROSS THE ARRAY PORT

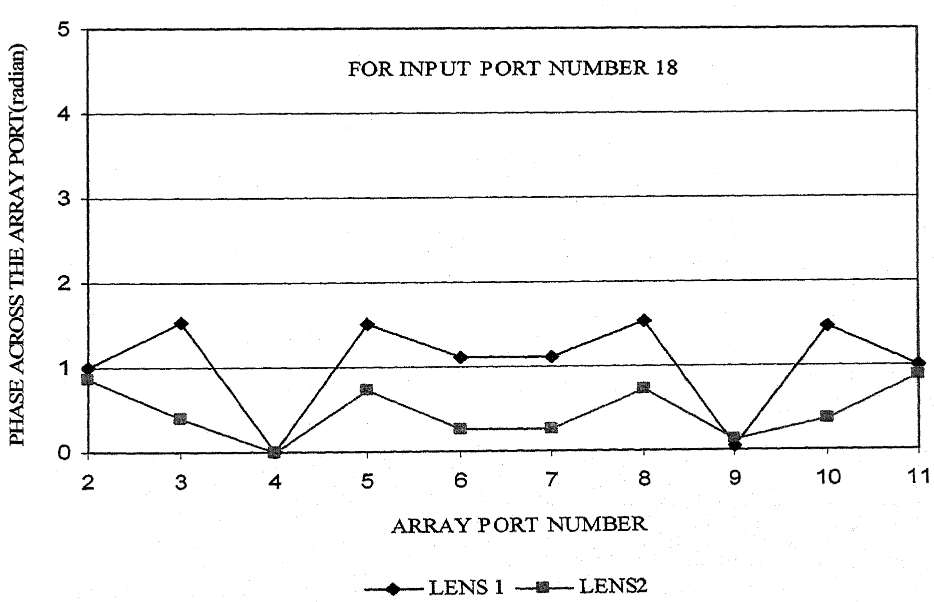

FIGURE 2.15(e) PHASE DISTRIBUTION ACROSS THE ARRAY

Table 2.1 and table 2.2 show the coupling coefficient from input ports to input ports and output ports to output ports.

TABLE 2.1: Coupling from inputs ports to input ports and output ports to output ports

For Rotman lens1

INPU PORT NO.	COUPLING COEFFICIENT(dB)	OUTPUT PORTS NO.	COUPLING COEFFICIENT(dB)
14-15	-11.78	2-3	-23.22
14-16	-12.38	2-4	-16.31
14-17	-11.30	2-5	-17.10
14-18	-16.93	2-6	-29.17
14-19	-20.43	2-7	-17.50
14-20	-21.65	2-8	-26.97
14-21	-15.93	2-9	-31.97
14-22	-10.86	2-10	-35.01
15-16	-14.49	2-11	-12.05
15-17	-17.95	3-4	-13.24
15-18	-21.67	3-5	-22.19
15-19	-35.73	3-6	-16.65
15-20	-24.42	3-7	-18.25
15-21	-17.37	3-8	-23.88
15-22	-15.39	3-9	-19.66
16-17	-22.93	3-10	-17.17
16-18	-23.98	3-11	-33.47
16-19	-25.84	4-5	-9.82
16-20	-22.65	4-6	-15.69
16-21	-23.92	4-7	-26.25
16-22	-18.93	4-8	-27.34
17-18	-21.18	4-9	-16.35
17-19	-20.56	4-10	-19.16
17-20	-26.51	4-11	-32.61
17-21	-30.76	5-6	-15.34
17-22	-19.92	5-7	-24.60
18-19	-21.03	5-8	-12.98
18-20	-24.71	5-9	-28.33
18-21	-20.91	5-10	-24.16
18-22	-16.83	5-11	-26.63
		6-7	-9.49
		6-8	-23.79
		6-9	-26.55
		6-10	-18.37
		6-11	-17.99

TABLE 2.2: Coupling from input ports to input ports and output ports to output ports for Rotman lens2

INPUT PORT NO.	COUPLING COEFFICIENT(dB)	OUTPUT PORTS NO.	COUPLING COEFFICIENT(dB)
14-15	-22.82	2-3	-12.05
14-16	-13.00	2-4	-16.62
14-17	-14.36	2-5	-24.22
14-18	-14.73	2-6	-20.64
14-19	-13.85	2-7	-18.75
14-20	-20.45	2-8	-24.39
14-21	-17.87	2-9	-19.46
14-22	-8.99	2-10	-23.63
15-16	-21.64	2-11	-13.68
15-17	-21.15	3-4	-13.15
15-18	-17.90	3-5	-26.38
15-19	-26.55	3-6	-16.52
15-20	-19.08	3-7	-17.13
15-21	-17.20	3-8	-24.19
15-22	-15.27	3-9	-16.82
16-17	-16.18	3-10	-17.14
16-18	-23.66	3-11	-23.18
16-19	-19.87	4-5	-10.54
16-20	-22.37	4-6	-16.02
16-21	-18.33	4-7	-26.99
16-22	-17.19	4-8	-25.82
17-18	-12.94	4-9	-15.69
17-19	-19.65	4-10	-16.39
17-20	-19.93	4-11	-19.42
17-21	-23.69	5-6	-18.64
17-22	-12.75	5-7	-26.46
18-19	-12.83	5-8	-10.62
18-20	-26.22	5-9	-26.92
18-21	-18.03	5-10	-26.00
18-22	-14.30	5-11	-25.87
		6-7	-11.01
		6-8	-24.35
		6-9	-25.18
		6-10	-16.43
		6-11	-19.34

The percentage of power distributed among various ports for both the lenses are given in the table 2.3, for lens 1, g = 1.74 and lens 2, g = 1.186 and other parameters are same for both lenses. Since as the value of "g" increases curvature of the feed contour increases and the size of lens also increases, for lens 2 more power is lost in the lens as its size is large. Also for lens 2 curvature of the feed contour is more, therefore, it is coupling more power back towards feed ports.

TABLE 2.3: Percentage of power distributed among various ports

FEED PORT NO.	PERCENTAGE OF POWER REFLECTED	PERCENTAGE OF POWER LOST IN DUMMY PORTS	PERCENTAGE OF POWER GOING TO ANTENNA ARRAY	PERCENTAGE OF POWER COUPLED TO FEED PORTS	PERCENTAGE OF POWER LOST IN LENS
Lens1					
14	0.56	9.63	41.39	19.64	28.78
15	0.66	11.82	53.63	16.87	17.02
16	4.41	7.83	59.94	16.10	11.72
17	10.89	7.38	53.97	22.00	5.76
18	12.96	3.66	60.66	19.84	2.88
Average	5.89	8.06	53.91	25.97	6.17
Lens2					
14	3.24	6.31	41.69	33.92	14.84
15	4.84	8.58	57.02	13.82	15.74
16	5.76	11.63	51.63	17.81	13.17
17	8.41	6.96	52.22	27.03	5.38
18	6.74	1.41	57.98	26.69	7.16
Average	5.79	6.97	52.10	23.85	11.25

Table 2.4 shows the direction of main beam, beam width and side lobe level for Rotman lens. The beam width for lens 2 is larger than lens 1.

TABLE 2.4: Direction of main beam, beam width and side lobe level for Rotman lens

FEED PORT NO.	DIRECTION OF MAIN BEAM IN DEGREE	BEAM WIDTH IN DEGREE	SIDE LOBE LEVEL IN dB
Lens1			
14	-30.00	17.00	-13.33
15	-22.00	16.00	-15.42
16	-14.00	15.00	-13.43
17	-8.00	15.00	-13.60
18	00	14.00	-13.85
Lens2			
14	-31.00	33.00	-14.31
15	-23.00	29.00	-11.99
16	-16.00	28.00	-10.48
17	-7.50	27.00	-12.41
18	00	26.00	-11.33

Figure 2.16 and figure 2.17 shows the radiation pattern obtained for g = 1.74 and g = 1.186 respectively. The beam crossover level obtained for the both the lenses are same (6 dB approximately). There is slight difference (1.0 degree) in the direction of main beam for both the lens. 3 dB beamwidth and sidelobe level for both the lenses are also different. The radiation pattern for both the design lenses reveals that the directions of beam maxima are different from the desired value. For input at port 14 the direction of main beam should be -35 degrees, whereas it is -31 and -30 degrees. Similarly interpretation may be applied for other input ports. Therefore modifications in the design approach are given in chapter 3 and 4.

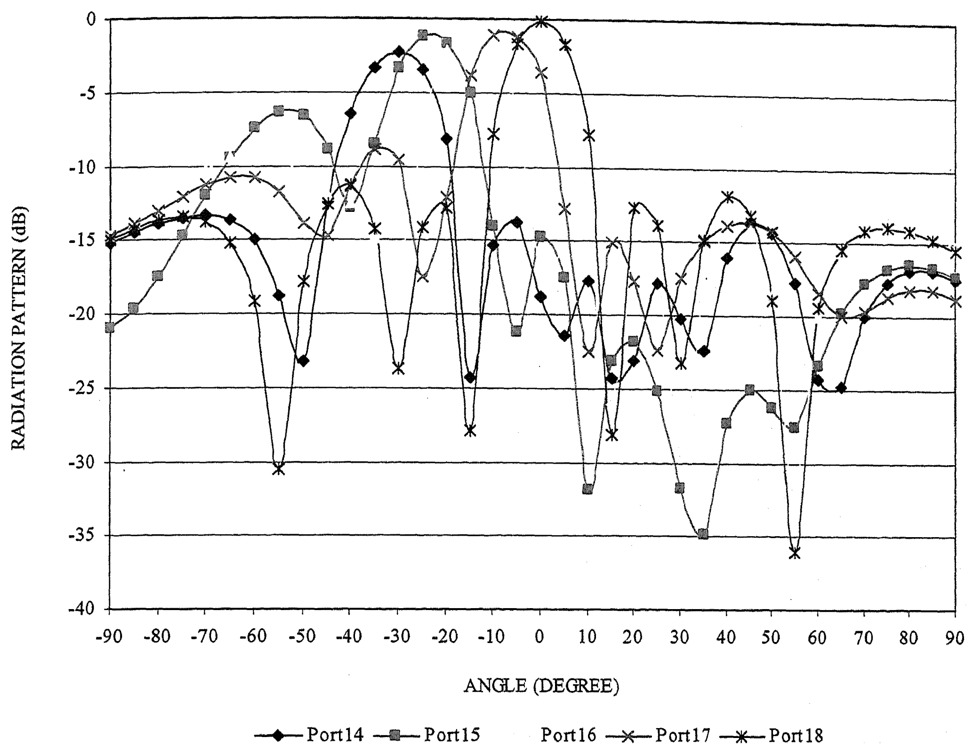

FIGURE 2.16 RADIATION PATTERN FOR ROTMAN LENS 1

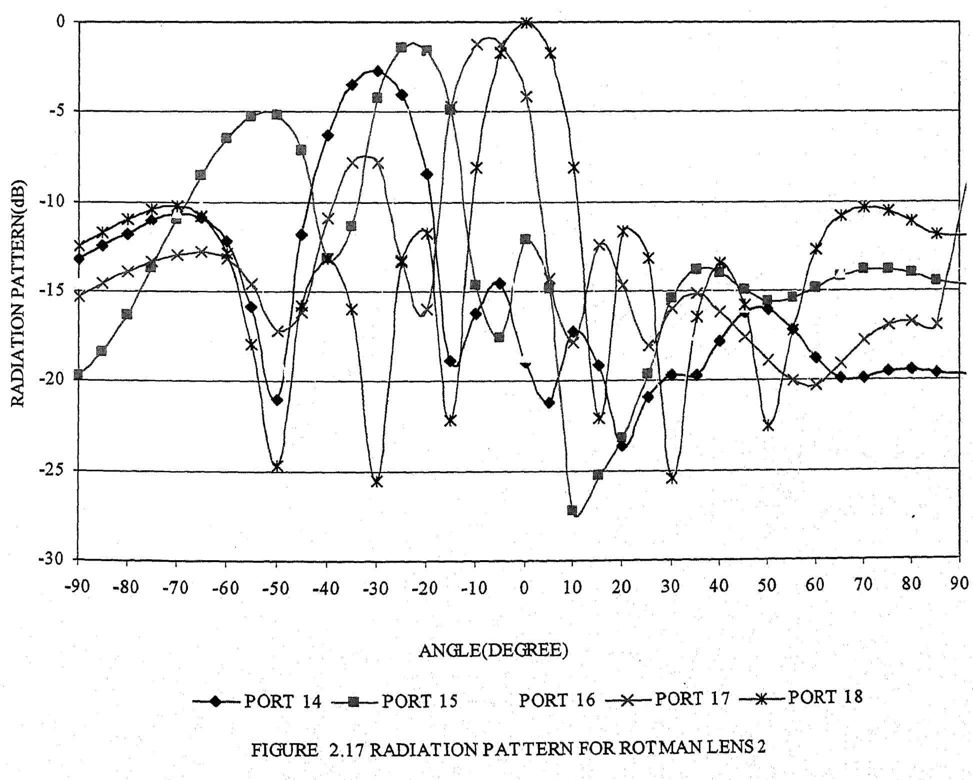

FIGURE 2.17 RADIATION PATTERN FOR ROTMAN LENS 2

2.6 CONCLUDING REMARK

A modified approach to design the Rotman type lens has been proposed. The work reported in the preceding section reveals a guideline for lens design. This is summarized in the following.

1. As the value of focal angle α increase, array contour closes and feed contour opens. As α increases height of feed contour also increases. Path length error also depends upon α, as α approaches towards scanning angle (θ), path length error decreases.
2. Lens aperture η determines the height of array contour and spacing between array elements. Spacing between array elements controls the appearance of grating lobes. Therefore spacing between array elements should not be greater than a certain limit.
3. Increasing 'g' has reverse effect to that with the increase in α. Small value of 'g' gives a compact lens and spillover losses reduce. Path length error also depends upon 'g' and it is minimum for a specific value of 'g'. Hence the value of 'g' should be selected keeping in view the requirement of equal height of both the contours, spillover losses and path length error.
4. The off axis focal length controls the dimension of the lens. It should be selected in such a manner that the normalized lens aperture η is less than 0.6. Since the path length error increases as η increases.

Repetitive iteration may be made to select the proper value of lens design parameters α, η and g.

Software has been used to design and analyze the lens using two dimensional electromagnetic field analysis methods. The result of analysis, namely reflection coefficient, radiation patterns of the antenna array, scattering matrix and power distribution in ports have been presented. The proposed analysis approach is well-suited for modification of the lens design to achieve improved performance and for implementing of CAD for the design of beam-forming lenses.

CHAPTER THREE

MODIFIED APPROACHE TO THE DESIGN OF ROTMAN TYPE MULTIPLE BEAM FORMING LENS

Design and analysis of Rotman lens have been given in previous chapters. Design approach for this lens is based on geometrical ray optics techniques. Katagi [8] suggested an improved method to design Rotman lens. Lens obtained using the approach suggested in [8] in terms as Katagi lens. In this chapter Rotman lens is designed using the approach suggested in [8] for the same requirements as Rotman lens in chapter 2 and analyzed using two dimensional analysis approaches.

3.1 LENS GEOMETRY

Figure 3.1 shows [8] the cross section of a Rotman lens. $\sum_1$ and $\sum_2$ are curves along which exciting elements and receiving elements are arranged respectively. Three focal points F_1, F_0 and F_2 are located on a circular arc at focal angle α, 0 and $-\alpha$ respectively. β is an angle of the direction of the main beam corresponding to a focal point F_1 whose angular position is designated by α. The aperture length of a linear array antenna is $2N_{MAX}$.

Basic difference between Rotman lens and Katagi lens is that a new design variable $\bar{\eta}$ is introduced and the phase error on the aperture of the linear array antenna is minimized. By introducing a design variable $\bar{\eta}$, relationship between design parameters for realizing a Rotman lens is derived and this improved method makes it possible to design a small and low loss Rotman lens antenna.

By using the procedure as that in [2], relations which determine the shape of $\sum_2$ are given by [8].

$$x = \frac{1}{g - a_0}\left[(g-1)w + b_0^2\bar{\eta}^2/2\right]f \tag{3.1}$$

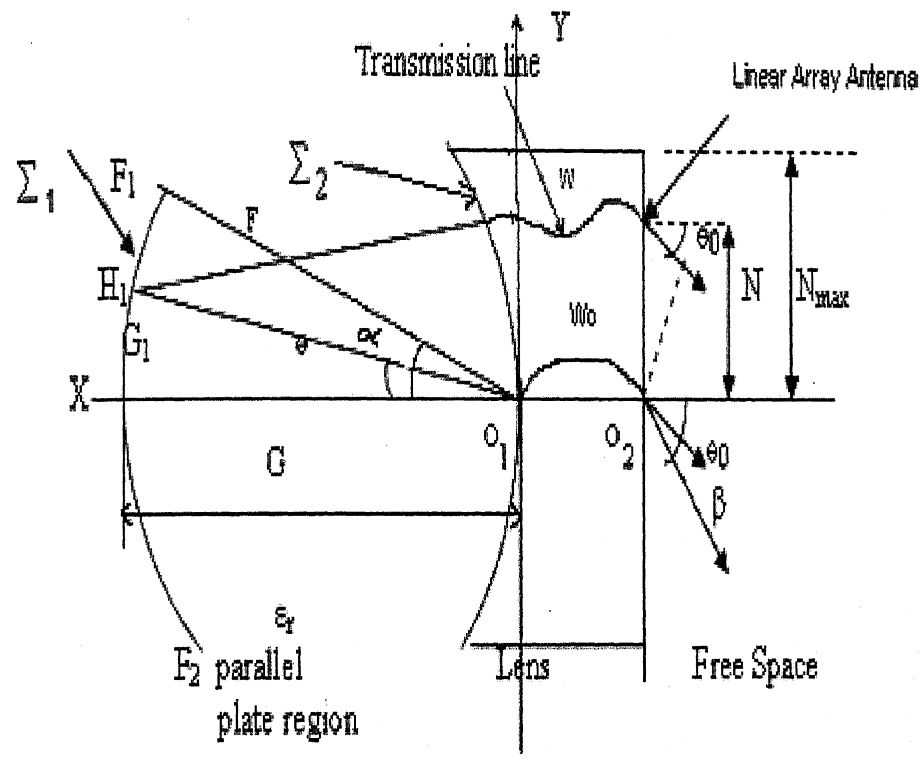

FIGURE 3.1: CROSS SECTION OF THE ROTMAN LENS

$$y = \bar{\eta}(1-w)f \tag{3.2}$$

Where $x = \frac{x}{N_{max}}, y = \frac{y}{N_{max}}$ (3.3)

$$g = \frac{G}{F}, f = \frac{F}{N_{max}} \tag{3.4}$$

$$\bar{\eta} = \frac{1}{\sqrt{\varepsilon\gamma}}\frac{b_1}{b_0}\frac{n}{f} \tag{3.5}$$

$$a_0 = \cos\alpha, b_0 = \sin\alpha, b_1 = \sin\beta \tag{3.6}$$

$$n = \frac{N}{N_{MAX}}, (|n| \leq 1) \tag{3.7}$$

$$w = \frac{W - W_0}{N_{\max} k} \frac{1}{f} \tag{3.8}$$

$$w = \frac{-b \pm \sqrt{b^2 - 4ac}}{2a} \tag{3.9}$$

$$a = 1 - \bar{\eta}^2 \left(\frac{g-1}{g-a_0} \right)^2 \tag{3.10}$$

$$b = 2g \frac{a_0 - 1}{g - a_0} - \frac{g-1}{(g-a_0)^2} b_0^2 \bar{\eta}^2 + 2\eta^2 - 2g \tag{3.11}$$

$$c = \frac{g b_0^2 \bar{\eta}^2}{g - a_0} - \frac{b_0^4 \bar{\eta}^4}{4(g-a_0)^2} - \bar{\eta}^2 \tag{3.12}$$

Where k is a wave number.

3.2 TWO DIMENSIONAL FIELD ANALYSIS OF ROTMAN LENS ANTENNA

It is required to design the lens for the following parameters

Angular Coverage = $\pm$ 35 degree

Number of antenna elements = 10

Number of input beams = 09

Center frequency = 3464.1 MHz

The lens is assumed to be fabricated in microstrip version on a substrate of dielectric constant $\varepsilon_r = 3.7$, thickness 1/16 inches, and lost tangent 0.001.

To fulfill the above requirements, the following design parameters are selected

Focal angle $\alpha = 35$ degree

Off axis focal length $F = 2.7\,\lambda$

Rotman and turner [3] described a procedure for estimating the optimum value of 'g'(ratio of on axis to off axis focal length) for a given choice of the off axis focal angle α.

For $\alpha = 35$ degrees,

$g = 1 + \alpha^2 / 2 = 1.186$

$\eta = 0.58$ (Antenna spacing element = 1.2 inches) is selected

In the design lens same port number notation are used as shown in figure 2.11.

3.3 RESULT AND DISCUSSION

Figure 3.2 shows the reflection coefficient at the input ports for the improved designed method [8], so called Katagi lens. The Reflection coefficients for Katagi lens are much smaller than Rotman lens.

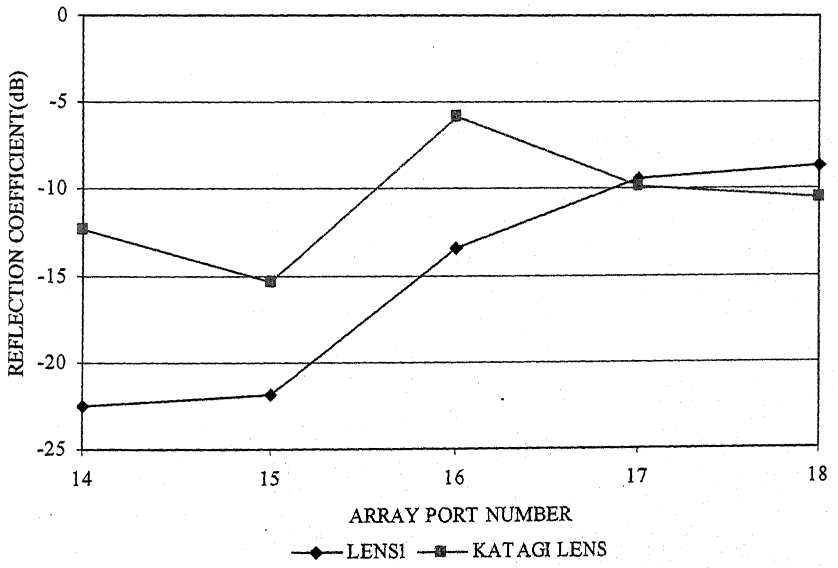

FIGURE 3.2 REFLECTION COEFFICIENT AT INPUT PORTS FOR KATAGI LENS

Amplitude distribution across the array ports for input at different ports are shown in figure 3.3(a)-3.3(e). When inputs apply at port number 15 the coupling coefficient is minimum at port number 10 for lens1 and at port number 9 for Katagi lens. When input applies at port number 15 the coupling coefficient is minimum at port number 5 for lens1 and port number 6 for Katagi lens. When input apply at port number 16 the coupling coefficient is minimum at port number 8 for lens1 and port number 6 for Katagi lens. When input applies at port number 17 the coupling coefficient is minimum at port number 6 for

lens1 and port number 4 for Katagi lens. When input applies at port number 18 the coupling coefficient is minimum at port number 6 for lens1 and port number 5 for Katagi lens.

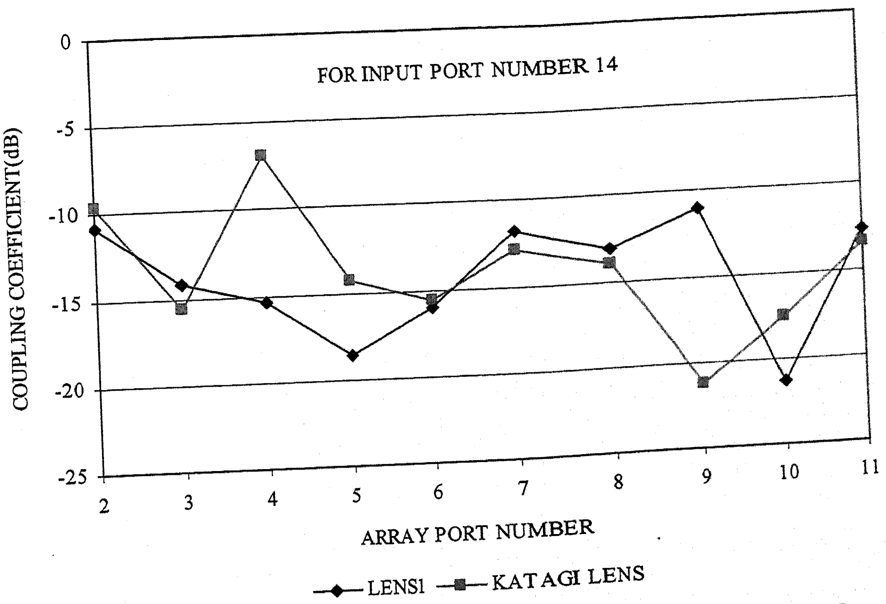

FIGURE 3.3(a) AMPLITUDE DISTRIBUTION ACROSS THE ARRAY PORTS

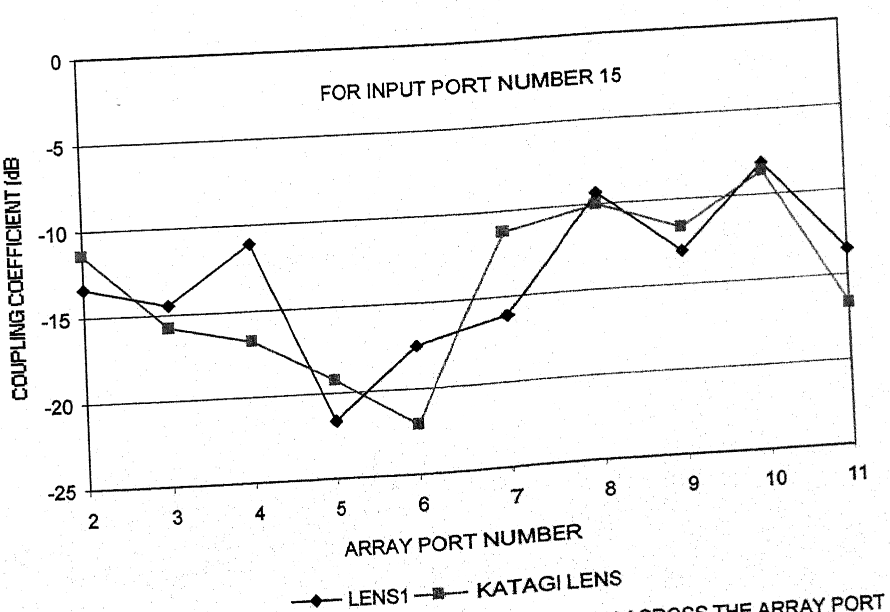

FIGURE 3.3(b) AMPLITUDE DISTRIBUTION ACROSS THE ARRAY PORT

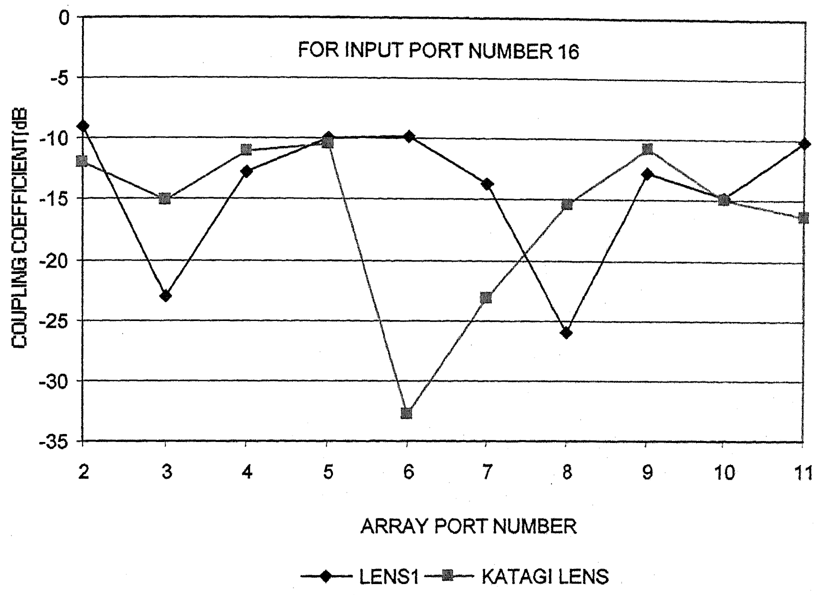

FIGURE 3.3(c) AMPLITUDE DISTRIBUTION ACROSS THE ARRAY PORTS

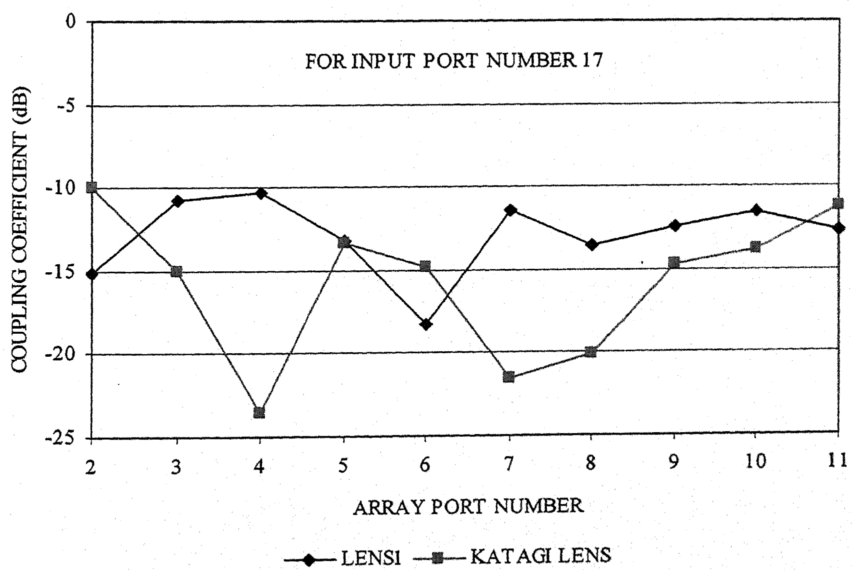

FIGURE 3.3(d) AMLITUDE DISTRIBUTION ACROSS THE ARRAY PORTS

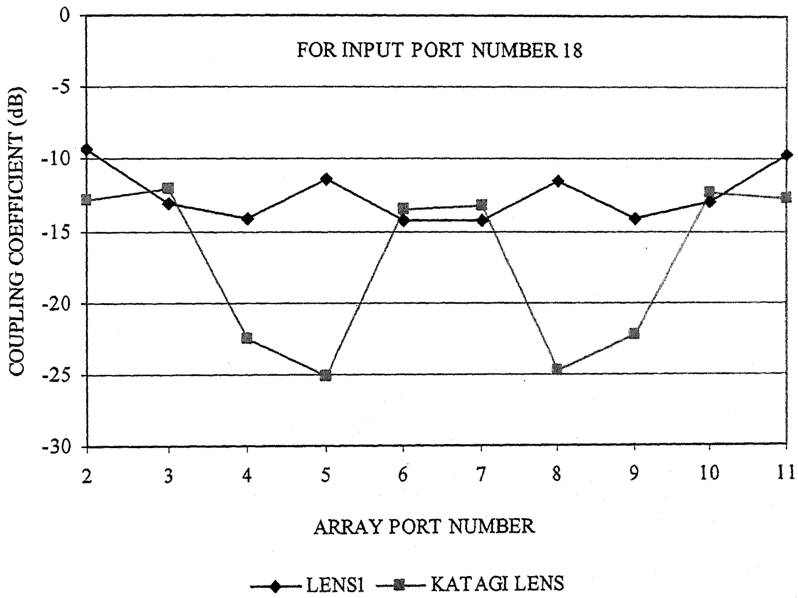

FIGURE 3.3(e) AMPLITUDE DISTRIBUTION ACROSS THE ARRAY PORTS

Figure 3.4(a)-3.4(e) shows the phase distribution across the array ports for both the lenses. For the input at port number 14, the phase variation across the array port is approximately two radians. For the input at port number 15, the phase variation across the array ports is approximately three radians. For the input at port number 16, the phase variation is approximately five radians. For input at port number 17, the phase variation is approximately one radian. For input port number 18, the phase distribution minimum at port number (6, 7) for katagi lens and port number (4, 9) for lens1.

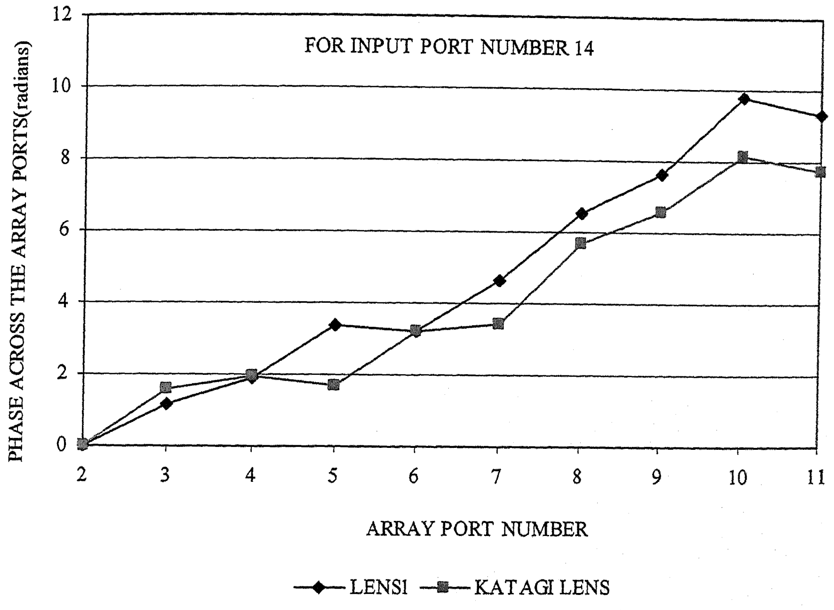

FIGURE 3.4(a) PHASE DISTRIBUTION ACROSS THE ARRAY PORTS

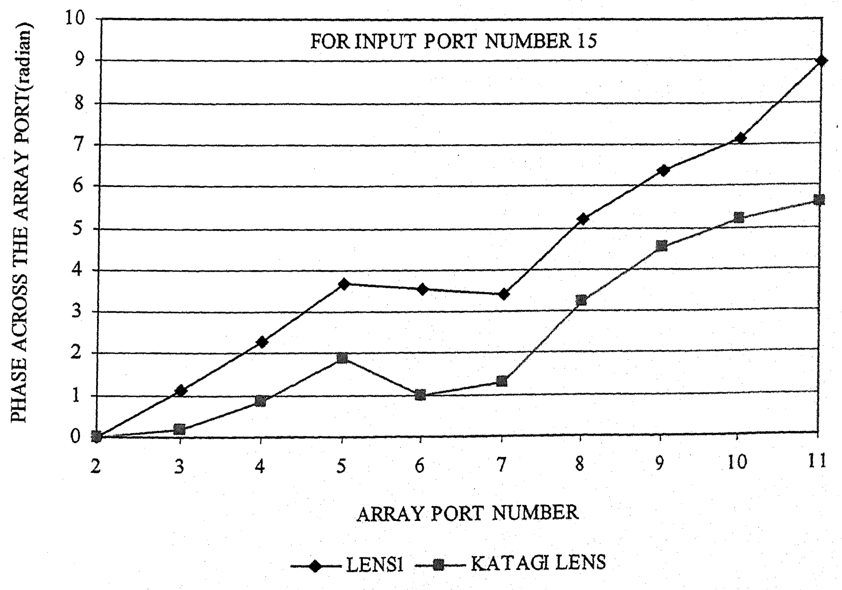

FIGURE 3.4(b) PHASE DISTRIBUTION ACROSS THE ARRAY PORTS

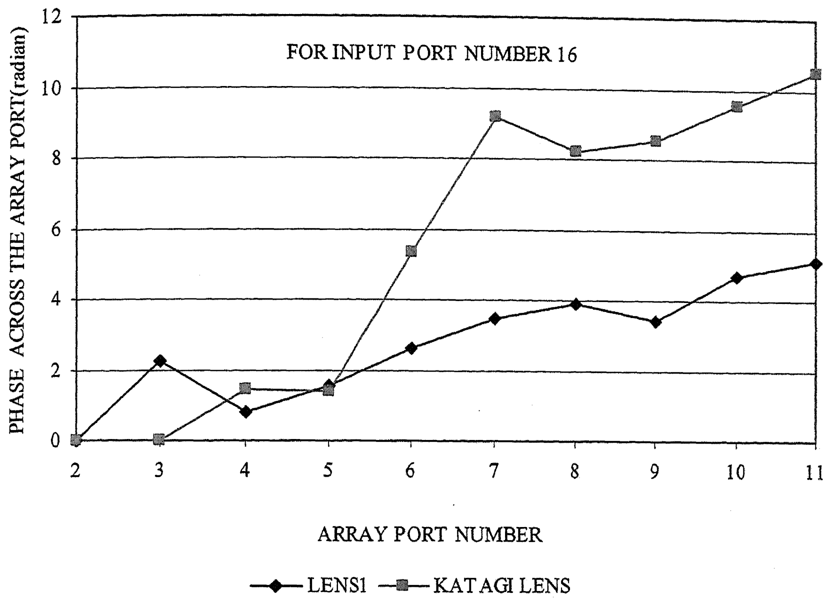

FIGURE 3.4(c) PHASE DISTRIBUTION ACROSS THE ARRAY PORT

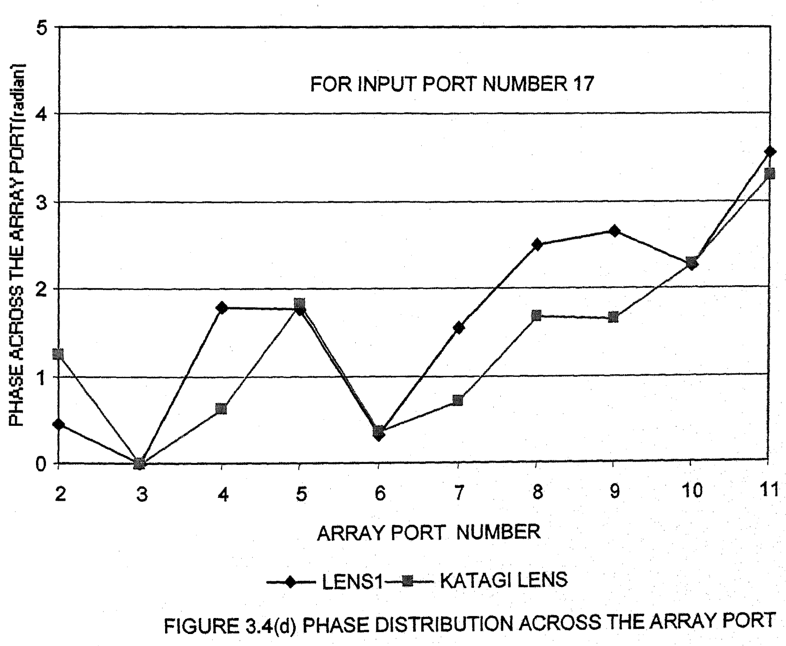

FIGURE 3.4(d) PHASE DISTRIBUTION ACROSS THE ARRAY PORT

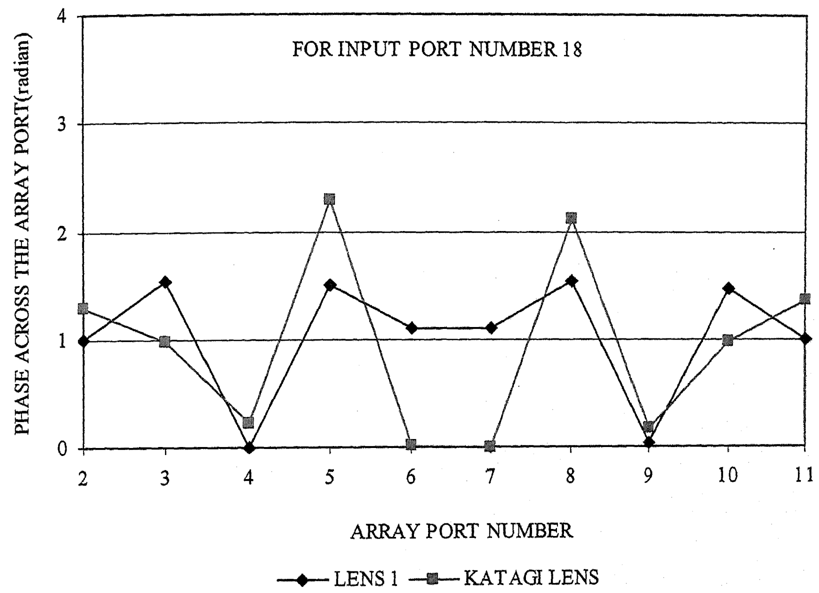

FIGURE 3.4(e) PHASE DISTRIBUTION ACROSS THE ARRAY PORT

Table 3.1 shows the coupling coefficients from input ports to input ports and output ports to output ports for Katagi lens.

Table 3.2 shows the percentage of power distributed among various ports for lens. This table revels that:

1. Average percentage of power lost in dummy ports for Katagi lens is much higher than the Rotman lens.
2. Average percentage of power reflected back in Katagi lens is large.
3. Power coupled back to the feed ports for lens1 is larger than the Katagi lens.

TABLE 3.1: Coupling from input ports to input ports and output ports to output ports for Katagi lens

Input Port No.	Coupling Coefficient (dB)	Output Ports No.	Coupling Coefficient (dB)
14-15	-17.58	2-3	-9.56
14-16	-18.80	2-4	-26.36
14-17	-23.84	2-5	-16.53
14-18	-15.64	2-6	-23.64
14-19	-26.56	2-7	-37.49
14-20	-24.82	2-8	-26.88
14-21	-15.65	2-9	-26.39
14-22	-10.22	2-10	-29.48
15-16	-15.36	2-11	-21.33
15-17	-16.97	3-4	-10.94
15-18	-15.72	3-5	-12.73
15-19	-17.66	3-6	-19.06
15-20	-24.21	3-7	-20.03
15-21	-25.09	3-8	-30.39
15-22	-8.71	3-9	-26.21
16-17	-16.29	3-10	-28.66
16-18	-19.41	3-11	-28.85
16-19	-20.55	4-5	-10.87
16-20	-14.52	4-6	-19.87
16-21	-21.95	4-7	-18.42
16-22	-15.07	4-8	-28.75
17-18	-8.21	4-9	-23.36
17-19	-15.31	4-10	-27.06
17-20	-27.47	4-11	-28.69
17-21	-13.68	5-6	-10.64
17-22	-13.65	5-7	-23.15
18-19	-10.35	5-8	-22.90
18-20	-29.75	5-9	-26.33
18-21	-20.59	5-10	-33.64
18-22	-11.96	5-11	-28.80
		6-7	-12.59
		6-8	-23.39
		6-9	-19.20
		6-10	-20.25
		6-11	-31.75

Table 3.2: Percentage of power distributed among various ports.

Feed port No.	**Percentage of power reflected**	**Percentage of power lost in dummy ports**	**Percentage of power going to antenna array**	**Percentage of power coupled to feed ports**	**Percentage of power lost in lens**
Lens1					
14					
15	0.56	9.63	41.39	19.64	28.78
16	0.66	11.82	53.63	16.87	17.02
17	4.41	7.83	59.94	16.10	11.72
18	10.89	7.38	53.97	22.00	5.76
Average	12.96	3.66	60.66	19.84	2.88
	5.89	8.06	53.91	25.97	6.17
Katagi lens					
14	5.76	12.71	22.65	17.79	41.09
15	2.89	15.42	51.96	22.67	7.06
16	25	9.48	42.96	10.68	11.88
17	10.24	22.71	36.18	25.49	5.38
18	8.41	9.61	35.05	16.15	30.78
average	10.46	13.98	37.76	18.55	19.23

Table 3.3 shows the direction of main beam, beam width and side lobe level. For input at port 14, the direction of main beam is -32 degree for Katagi lens and for the Rotman lens is -30 degree. The beam widths for both the lenses are almost equal. The Side lobe level is minimum for Katagi lens.

Table 3.3: Direction of main beam, beam width and side lobe level

FEED PORT NO.	DIRECTION OF MAIN BEAM(DEG.)	BEAM WIDTH(DEG.)	SIDE LOBE LEVEL (DB)
Rotman Lens			
14	-30.00	17.00	-13.33
15	-22.00	16.00	-15.42
16	-14.00	15.00	-13.43
17	-8.00	15.00	-13.60
18	00	14.00	-13.85
Katagi lens			
14	-32.00	18.00	-26.65
15	-21.00	16.00	-31.09
16	-17.00	14.00	-34.60
17	-8.00	14.00	-19.01
18	0.00	14.00	-16.69

Figure 3.5 shows the radiation pattern for the Katagi lens. Radiation pattern obtained for Katagi lens have the characteristics close to as predicted by its design approach.

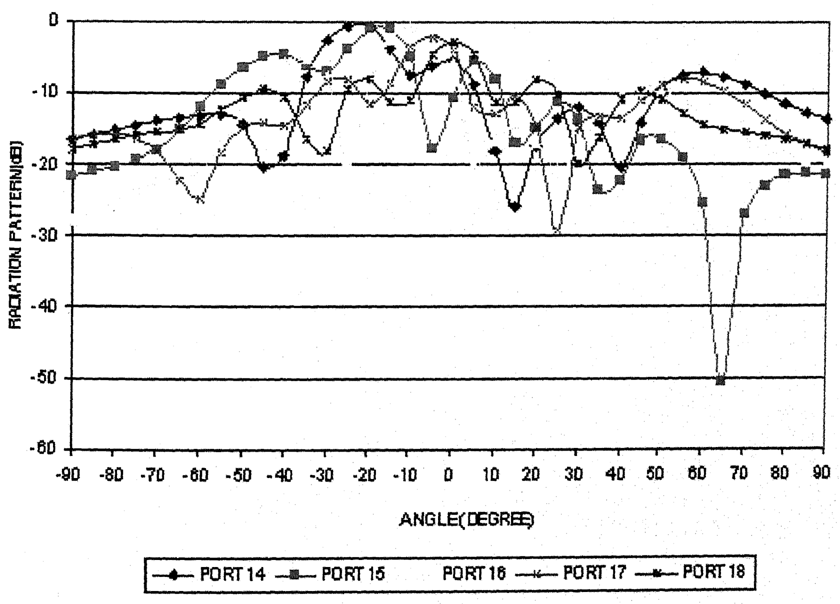

FIG. 3.5 RADIATION PATTERN FOR KATAGI LENS

3.4 CONCLUDING REMARKS:

A modified approach is used to design the Rotman lens1 and Katagi lens.The size of Rotman lens is large, so more power is lost in it. Also the curvature of the feed contour of Katagi lens is large. Therefore it is coupled more power back toward the feed ports.

CHAPTER FOUR

ELLIPTICAL REFOCUSSING OF ROTMAN LENS

Design and analysis of Rotman lens and Katagi lens have been given in previous chapters. In this chapter elliptical refocusing of Rotman lens is discussed for the same requirements as Rotman lens. Comparison of the results obtained from elliptical refocussed lens with those obtained for the Rotman lens is also given.

4.1 LENS GEOMETRY

Figure 4.1 shows the cross-section of a trifocal Rotman type lens. One focal point F_o is located on the central axis, and two others F_1 and F_2 are symmetrically located either side on a elliptical focal arc. Outer contour I_2 is a straight line and defines the position of the radiating elements. I_1 is the inner contour of the lens. The inner and outer contours are connected by TEM mode transmission lines W (N). Two off axis focal points $F_1$and F_2 are located on the focal arc at angle $+\alpha$ and $-\alpha$ respectively.

A ray originating from F_1 may reach the wave front through a general point P(X,Y) on the inner contour I_1 transmission line W(N) and point Q(N) on the contour, and then tracing a straight line at an angle $-\alpha$ and terminate perpendicular to the wave front. Also the ray from F_1 may reach the wave front from F_1 to the point O_1, and then through transmission line W(O) to the wave front. Similarly rays from other feed points may reach their respective wave front.

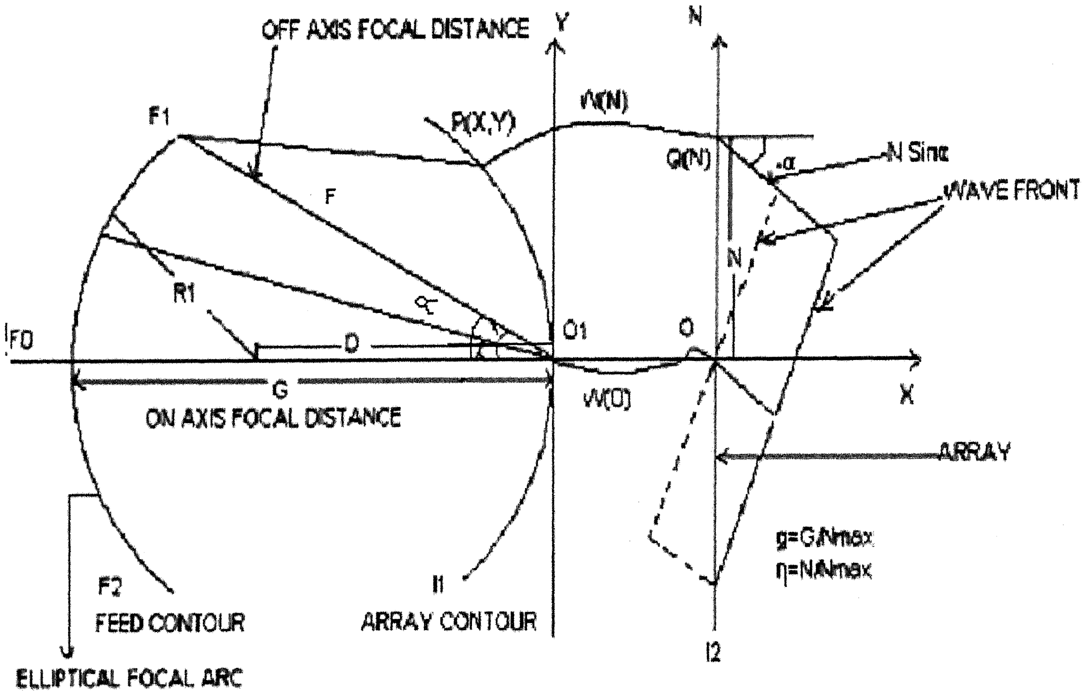

FIGURE 4.1: ELLIPTICALLY FOCUSED LENS

Inner contour and the transmission lines are designed from the design equations which are derived using the fact that, at the wave front, all the rays must be in phase independent of the path they travel. This requires that the total phase shift in traversing the path to reach the wave front in each case be equal. Using this concept and referring to figure 4.1 following design equations are written:

$$\varepsilon_r^{1/2} F_1P + \varepsilon_{re}^{1/2} W(N) + N \sin\alpha = \varepsilon_r^{1/2} F + \varepsilon_{re}^{1/2} W(O) \tag{4.1}$$

$$\varepsilon_r^{1/2} F_2P + \varepsilon_{re}^{1/2} W(N) - N \sin\alpha = \varepsilon_r^{1/2} F + \varepsilon_{re}^{1/2} W(O) \tag{4.2}$$

$$\varepsilon_r^{1/2} F_0P + \varepsilon_{re}^{1/2} W(N) = \varepsilon_r^{1/2} G + \varepsilon_{re}^{1/2} W(O) \tag{4.3}$$

Where, $(F_1P)^2 = (F\cos\alpha + X)^2 + (F\sin\alpha - Y)^2$

$$(F_2P)^2 = (F\cos\alpha + X)^2 + (F\sin\alpha + Y)^2$$

$$(F_0P)^2 = (G+X)^2 + (Y)^2$$

Algebraic manipulation of above equations leads to the following results

$$y = \eta\ \{1 - w\ \varepsilon_{re}^{1/2} / \varepsilon_r^{1/2}\} / \varepsilon_{re}^{1/2} \tag{4.4}$$

$$X = \{w(g-1)/a(a-g)\}\ \varepsilon_{re}^{1/2} / \varepsilon_r^{1/2} + \eta^2 b^2 / 2\ \varepsilon_r\ (a-g) \tag{4.5}$$

$$Aw^2 + B\,w + C = 0 \tag{4.6}$$

Where ,

$a = \cos\alpha$ $\quad b = \sin\alpha$ $\quad \eta = N/F$ $\quad x = X / F$

$y = Y/F$ $\quad g = G/F$ $\quad w = \{W(n) - W(0)\}/F$

$A = (g-1)^2\ \varepsilon_{re} / \{\ a-g)\}\ \varepsilon_r\ \} = \eta^2\ \varepsilon_{re} / \varepsilon_r^{\ 2} - \varepsilon_{re} / \varepsilon_r$

$B = b^2(g-1)\eta^2\ \varepsilon_{re}^{1/2} / \{(a-g)^2\ \varepsilon_r^{3/2}\} - 2\,\eta^2\ \varepsilon_{re}^{1/2}/\varepsilon_r^{3/2} + 2g(g-1)\varepsilon_{re}^{1/2}/\{(a-g)\varepsilon_r^{1/2}\} + 2g\varepsilon_{re}^{1/2}/\varepsilon_r^{1/2}$

$C = b^4 + \eta^4 / 4\ \varepsilon_r^{\ 2}(a-g)^2 + \eta^2 / \varepsilon_r + gb^2\ \eta^2\ \{\varepsilon_r(a-g)\}$

The equation to design array contour and transmission lines will be exactly the same as for the Rotman lens. Only difference will be in focal arc. The focal arc is given by the following equations.

$$\frac{X^2}{a^2} + \frac{Y^2}{b^2} = 1 \tag{4.7}$$

Where $b^2 = a^2(1 - e^2)$

$a^2 = F^2\{(1 - e^2\cos^2\alpha)/(1 - e^2)\}$

e = the eccentricity of the elliptical focal arc.

F = the off axis focal length, α is the focal angle.

ε_r = the dielectric constant of the lens substrate

ε_{re} = the effective dielectric constant of the transmission lines.

For the given value of design parameters α , F, g and ε_r , array contour and transmission lines W (N) can be designed using the above equations.

4.2 SPECIFIC DESIGN EXAMPLE

This section describes an example of the design and analysis of Rotman lens and elliptical refocussed lens to feed a linear array of waveguide horns. It is required to design the lens for the following requirements

Angular coverage = $\pm 25^0$

Number of antenna elements = 10

Number of input beams = 09

Central frequency = 3.4641 GHz

The complete structure is assumed to be fabricated in a microstrip substrate of thickness 1/16 inch and dielectric constant 3.7.The loss tangent is 0.001.

As per the guidelines recommended earlier following design parameters have been selected for the two lenses.

a. For Rotman lens

$g = 1.023$

$\alpha = 25^\circ$

$\eta = 0.58$ (antenna element spacing = 1.0 inch)

$F = 2.7\lambda$

b. For elliptical refocussed lens

$g = 1.014$

$\alpha = 25^\circ$

$\eta = 0.58$

$F = 2.7\lambda$

$e = 0.58$

4.3 RESULT AND DISCUSSION

Figure 4.2 shows the reflection coefficients at the input ports for the Rotman lens and elliptically refocussed lens. Reflection coefficient for the elliptical refocussed lens is much greater than the Rotman lens.

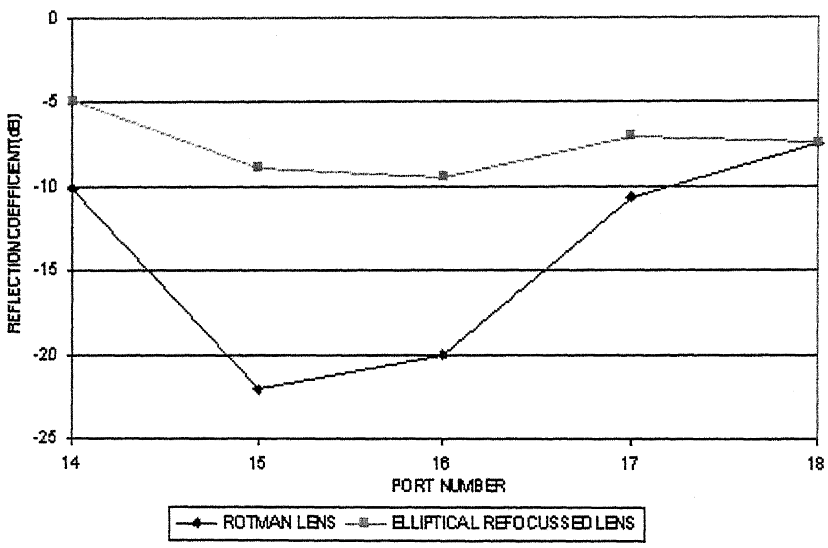

FIGURE 4.2 REFLECTION COEFFICENT AT INPUT PORTS

Amplitude distribution across the array ports for both the lenses is shown in figure 4.3(a) – 4.3(e). When input applies at port number 14 the coupling coefficient is minimum at port number 3 for Rotman lens and at port number 6 for elliptical refocussed lens. When input applies at port number 15 the coupling coefficient is minimum at port 6 for Rotman lens and at port 7 for elliptical refocussed lens. When input applies at port number 16 the coupling coefficients is minimum at port 6 for Rotman lens and at port 7 for elliptical refocussed lens. When input applies at port number 17 the coupling coefficient is minimum at port 4 for Rotman lens and at port 7 for elliptical refocussed lens. When input applies at

port number 18 the coupling coefficient is minimum at port 5 for Rotman lens and port 7 for elliptical refocussed lens.

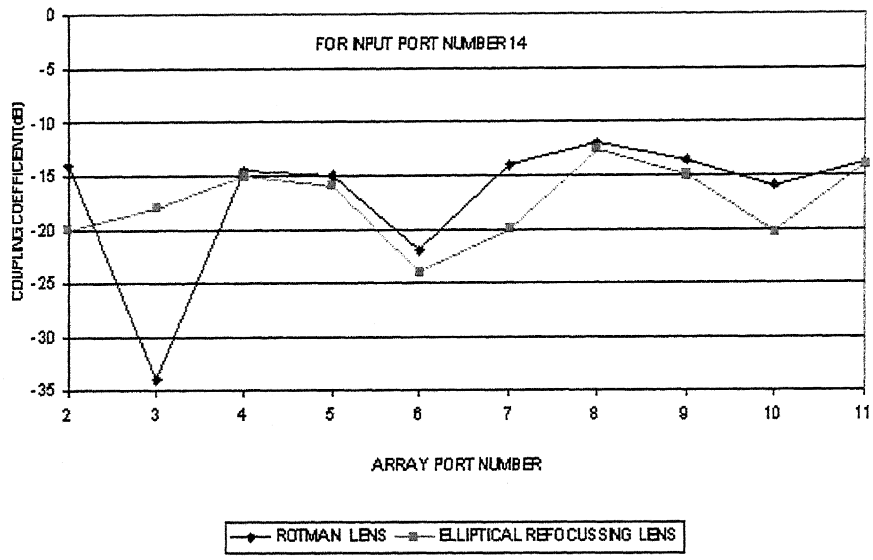

FIGURE 4.3(a) AMPLITUDE DISTRIBUTION ACROSS THE ARRAY PORT

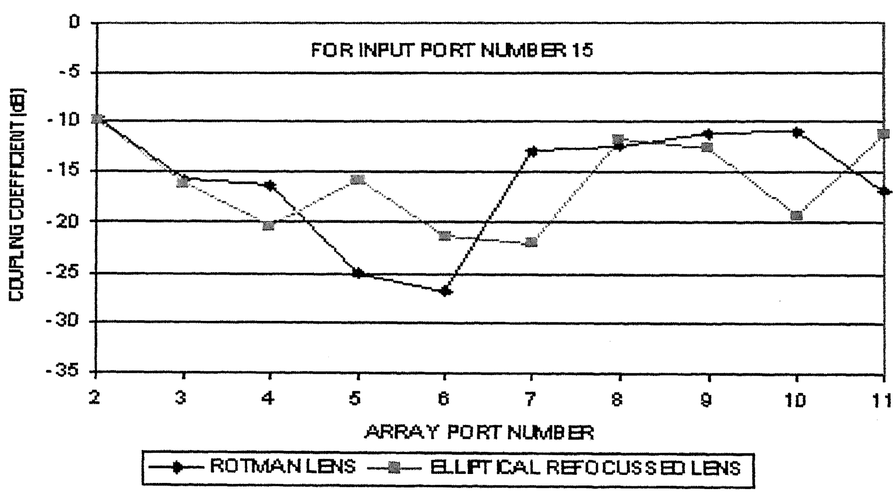

FIGURE4.3(b) AMPLITUDE DISTRIBUTION ACROSS ARRAY PORT

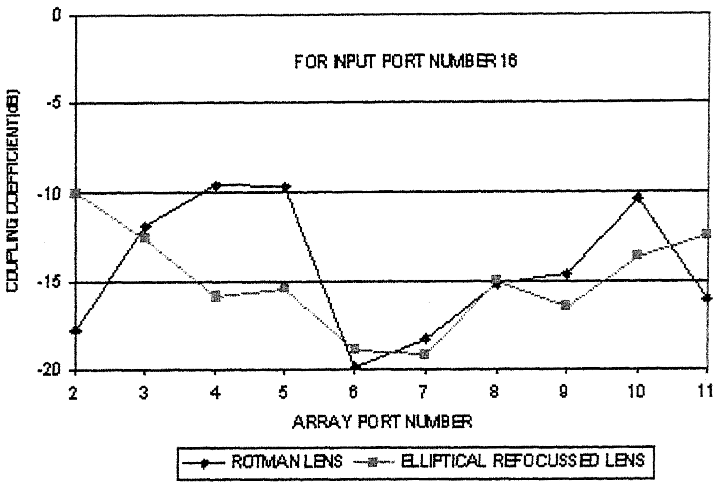

FIGURE 4.3(c) AMPLITUDE DISTRIBUTION ACROSS ARRAY PORT

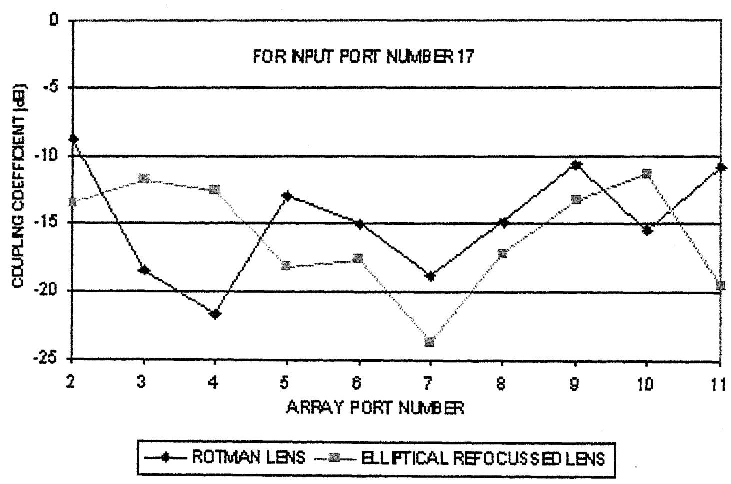

FIGURE 4.3(d) AMPLITUDE DISTRIBUTION ACROSS ARRAY PORT

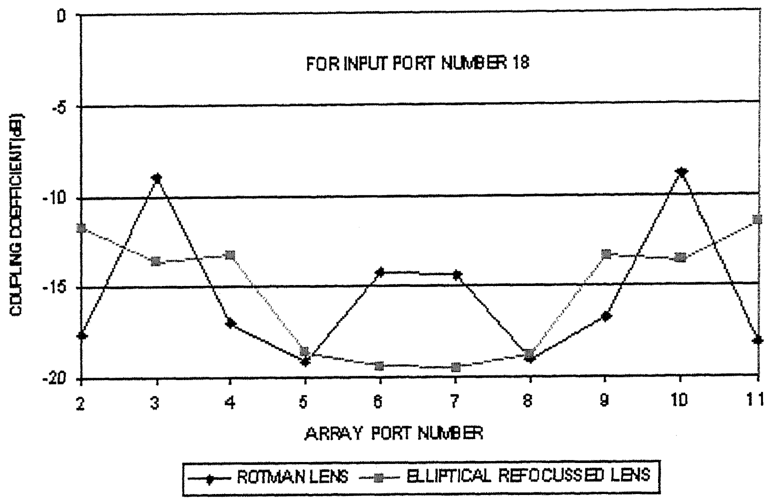

FIGURE 4.3(e) AMPLITUDE DISTRIBUTION ACROSS ARRAY PORT

Phase distribution across the array ports for both the lenses is shown in figure 4.4(a) – 4.4(e). For input port number 14, 15 and 16 the phase variation across the array port for approximately one radians. For input port number 17 and 18 the phase variation across the array port is approximately three radians.

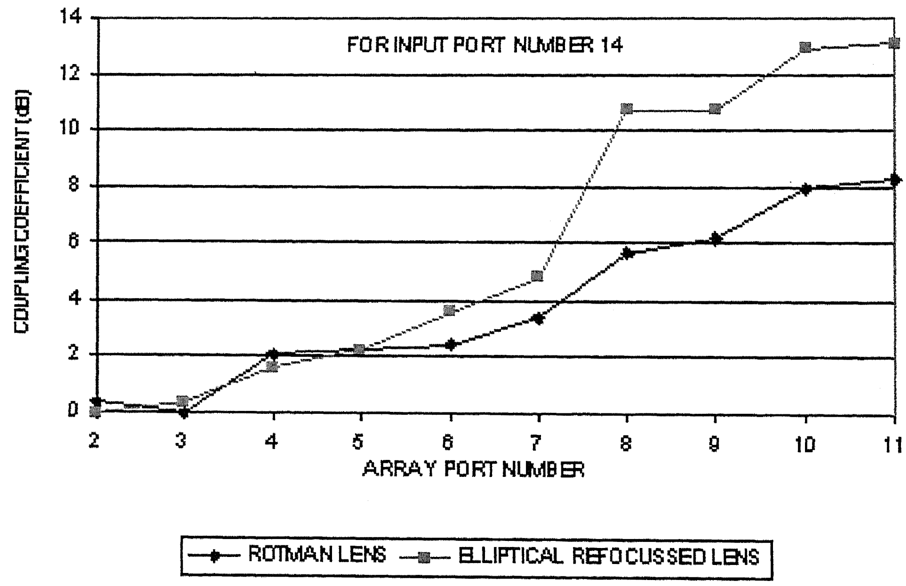

FIGURE 4.4(a) PHASE DISTRIBUTION ACROSS ARRAY PORT

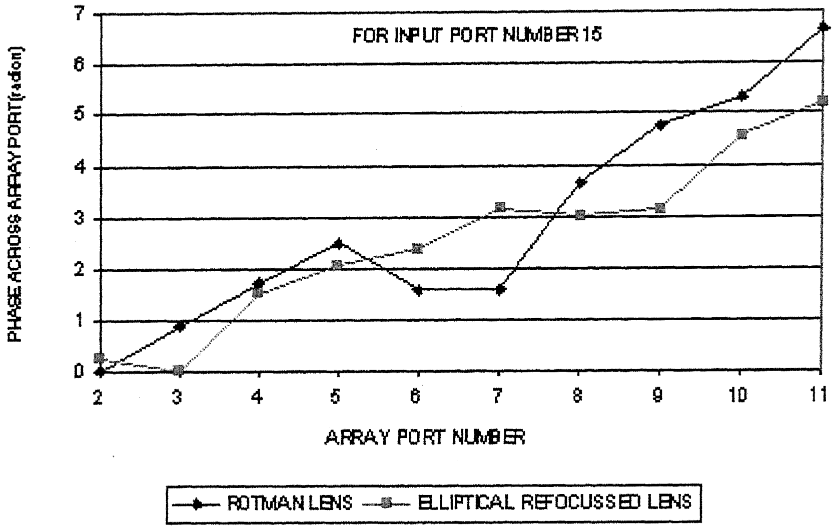

FIGURE4.4(b) PHASE DISTRIBUTION ACROSS ARRAY PORT

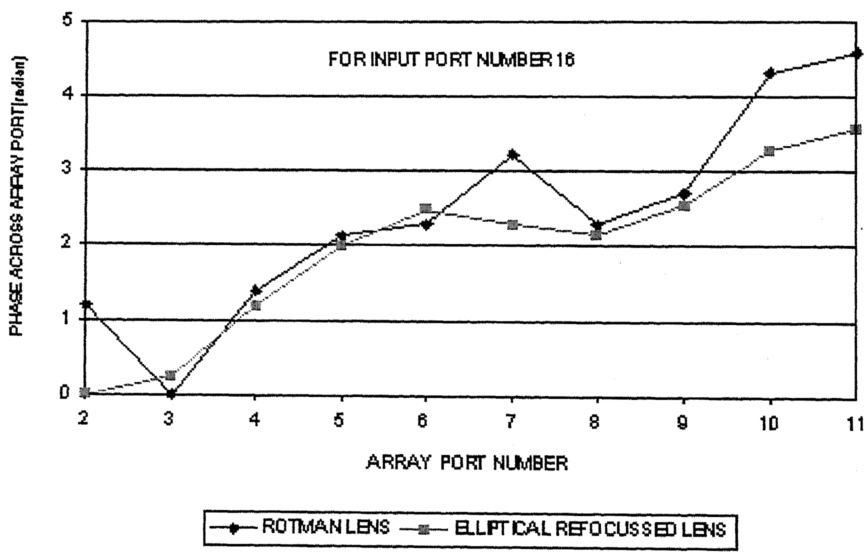

FIGURE4.4(c) PHASEDISTBUTIONACROSS ARRAY PORT

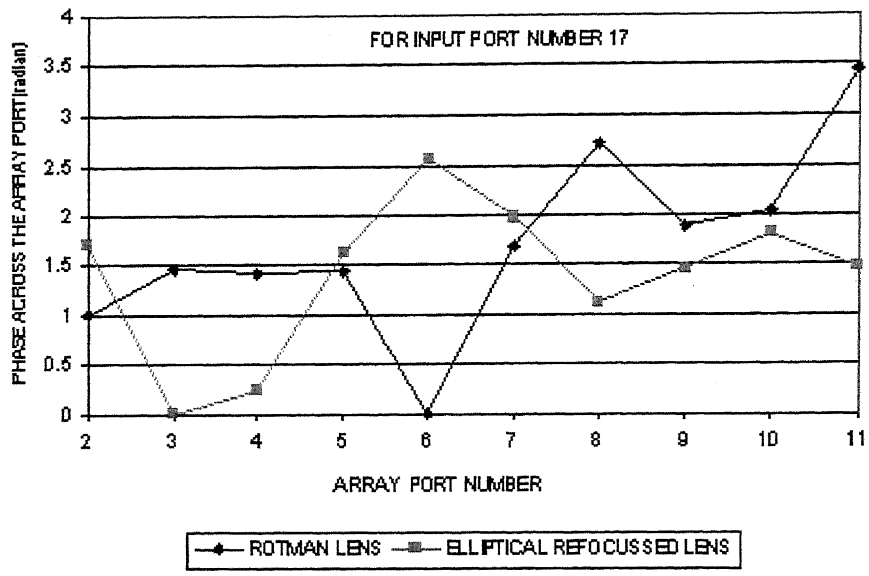

FIGURE4.4(d) PHASE DISTRIBUTION ACROSS ARRAY PORT

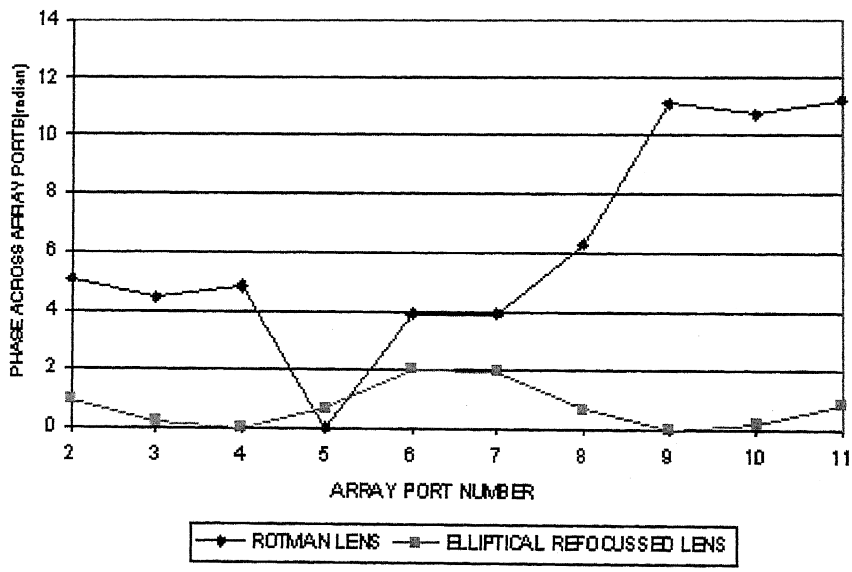

FIGURE4.4(e) PHASE DISTRIBUTION ACROSS THEARRAY PORT

Table 4.1 and 4.2 shows the coupling coefficients from input to inputs ports and output to output ports for Rotman lens and Elliptical refocussed lens respectively.

TABLE4.1: Coupling from inputs ports to input ports and output ports to output ports.

INPUT PORT NO.	COUPLING COEFFICIENT (dB)	OUTPUT PORT NO.	COUPLING COEFFICIENT (dB)
14-15	-13.05	2-3	-12.70
14-16	-11.62	2-4	-14.17
14-17	-9.43	2-5	-16.75
14-18	-18.20	2-6	-17.61
14-19	-28.83	2-7	-18.71
14-20	-21.74	2-8	-21.05
14-21	-17.16	2-9	-21.14
14-22	-9.29	2-10	-25.48
15-16	-9.61	2-11	-15.50
15-17	-12.46	3-4	-9.10
15-18	-13.64	3-5	-18.00
15-19	-14.91	3-6	-18.30
15-20	-15.83	3-7	-22.43
15-21	-16.09	3-8	-19.69
15-22	-15.92	3-9	-17.35
16-17	-22.91	3-10	-12.08
16-18	-19.66	3-11	25.78
16-19	-15.55	4-5	-11.37
16-20	-15.84	4-6	-14.62
16-21	-15.00	4-7	-33.13
16-22	-23.77	4-8	-16.80
17-18	-16.22	4-9	--21.12
17-19	-17.72	4-10	-16.88
17-20	-14.94	4-11	-21.31
17-21	-13.81	5-6	-13.73
17-22	-23.44	5-7	-30.88
18-19	-16.22	5-8	-15.28
18-20	-22.58	5-9	-16.86
18-21	-12.47	5-10	-20.06
18-22	-16.84	5-11	-21.58
		6-7	-9.31
		6-8	-30.07
		6-9	-32.03
		6-10	-22.63
		6-11	-19.48

TABLE 4.2: Coupling from inputs ports to input ports and output ports to output ports for elliptical refocussed lens.

INPUT PORT NO.	COUPLING COEFFICIENT (dB)	OUTPUT PORT NO.	COUPLING COEFFICIENT (dB)
14-15	-11.38	2-3	-7.82
14-16	-14.40	2-4	-25.25
14-17	-17.10	2-5	-15.25
14-18	-17.45	2-6	-23.02
14-19	-29.01	2-7	-26.23
14-20	-16.99	2-8	-17.75
14-21	-20.82	2-9	-21.63
14-22	-12.29	2-10	-19.40
15-16	-12.88	2-11	-19.44
15-17	-14.74	3-4	-9.53
15-18	-22.49	3-5	-14.81
15-19	-20.02	3-6	-19.99
15-20	-12.65	3-7	-30.78
15-21	-16.71	3-8	-25.57
15-22	-22.74	3-9	-21.16
16-17	-18.72	3-10	-21.24
16-18	-15.86	3-11	-19.30
16-19	-17.04	4-5	-12.20
16-20	-22.76	4-6	-16.36
16-21	-12.67	4-7	-25.29
16-22	-17.69	4-8	-18.35
17-18	-11.67	4-9	-14.43
17-19	-12.21	4-10	-21.27
17-20	-17.10	4-11	-22.73
17-21	-19.03	5-6	-17.47
17-22	-31.30	5-7	-24.08
18-19	-11.80	5-8	-17.90
18-20	-16.12	5-9	-18.32
18-21	-23.59	5-10	-26.47
18-22	-18.84	5-11	-18.35
		6-7	-15.71
		6-8	-26.28
		6-9	-25.80
		6-10	-30.21
		6-11	-26.94

Table 4.3 shows the percentage of power distributed among various ports for elliptical refocussed lens and Rotman lens. This table reveals that:

1. Percentage of power lost in dummy ports for Rotman lens is much less than elliptical refocussed lens
2. Percentage of power reflected by elliptical refocussed lens is large.
3. Power lost in the elliptical refocussed lens is less than the Rotman lens.
4. Percentage of power coupled back to feed ports for elliptical refocussed lens is less than the Rotman lens.

Table 4.3 Percentage of power distributed among various ports.

FEED PORT NO.	PERCENTAGE OF POWER REFLECTED	PERCENTAGE OF POWER LOST IN DUMMY PORTS	PERCENTAGE OF POWER GOING TO ANTENNA ARRAY	PERCENTAGE OF POWER COUPLED TO FEED PORTS	PERCENTAGE OF POWER LOST IN LENS
Rotman lens					
14	9.61	5.26	30.98	37.91	16.24
15	0.28	3.85	43.32	30.13	22.42
16	0.81	3.95	48.55	9.86	36.83
17	8.41	1.85	45.32	10.83	66.41
18	16.81	5.53	42.15	9.99	25.52
average	7.18	4.08	42.06	19.74	26.94
Elliptical refocussed Lens					
14	32.49	9.82	22.52	22.37	12.80
15	6.76	10.58	36.29	17.12	14.15
16	3.61	14.41	36.91	13.20	13.62
17	1.69	10.10	33.93	15.46	12.23
18	1.69	11.98	35.58	10.07	11.86
average	9.24	11.37	33.04	15.64	13.85

Figure 4.5 shows the radiation pattern for Rotman lens. Figure 4.6 shows the radiation pattern for elliptical refocussed lens. Radiation pattern obtained for elliptical refocussed have the characteristics close to as predicted by its design approach.

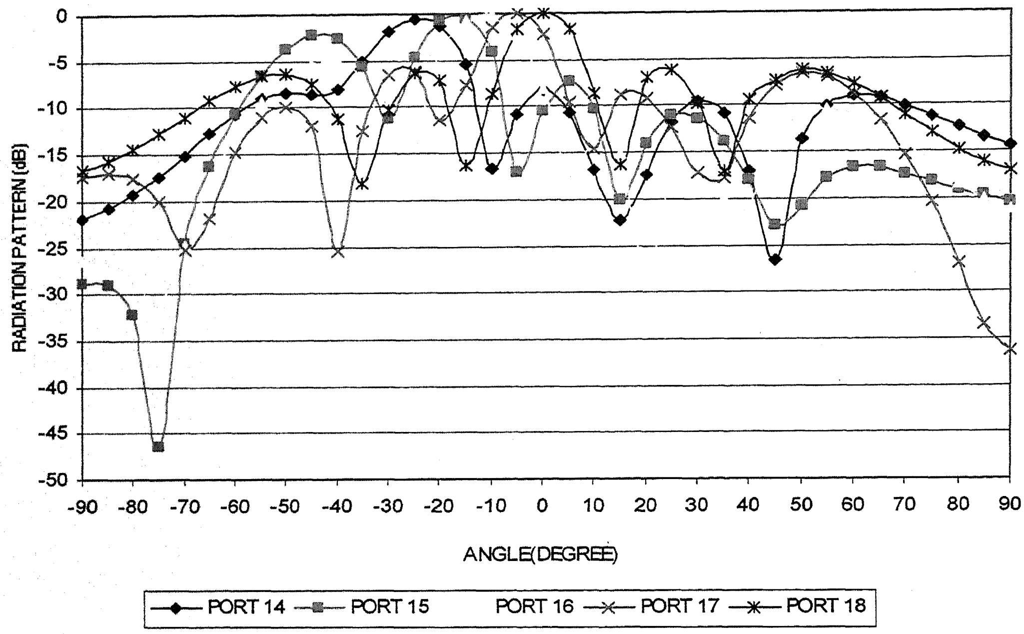

FIG. 4.5 RADIATION PATTERN FOR ROTMAN LENS

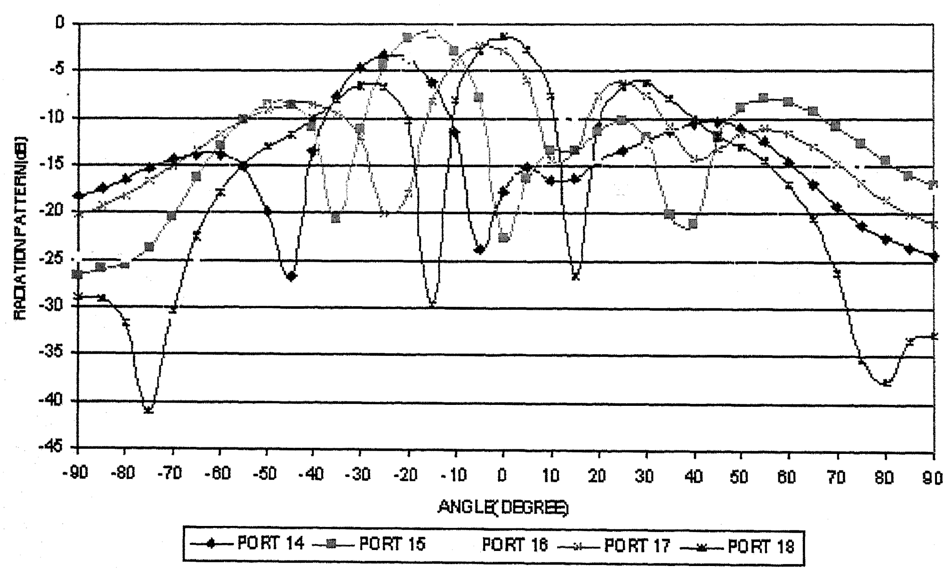

FIG 4.6 RADIATION PATTERN FOR ELLIPTICAL REFOCUSSED LENS

Table 4.4 shows the direction of main beam, beam width and side lobe level for Rotman lens. The direction of main beam for Rotman lens is 30 degree and for elliptical refocussed lens is 32 degree. The beam width for elliptical refocussed lens is larger than Rotman lens. The sidelobe level in elliptical refocussed lens is minimum.

Table 4.4 Direction of main beam, beam width, side lobe level for Rotman lens and elliptical refocusing lens.

FEED PORT NO.	DIRECTIONOF MAIN BEAM(DEG)	BEAM WIDTH(DEG)	SIDE LOBE LEVEL (dB)
Rotman Lens			
14	-30.00	17.00	-13.33
15	-22.00	16.00	-15.42
16	-14.00	15.00	-13.43
17	-8.00	15.00	-13.60
18	0.00	14.00	-13.85
Elliptical Refocussed Lens			
14	-32.00	18.00	-26.65
15	-21.00	16.00	-31.09
16	-17.00	14.00	-34.60
17	-8.00	14.00	-19.01
18	0.00	14.00	-16.69

4.4 CONCLUDING REMARKS

Design approach suggested into gives a lens in which all input ports are uniformly coupled to outports. The elliptical refocussed lens is designed for multiple beams forming are compared with Rotman lens. The percentage of power lost in elliptical refocussed lens is much less than the Rotman lens. The side lobe level in elliptical refocussed lens is minimum. The radiation pattern for elliptical refocusing lens is close to as predicated by its design approach.

CHAPTER FIVE

CONCLUDING REMARKS

A Rotman lens geometry suggested by Rotman and Turner [2] is a useful multiple beam forming network. Also it has advantages over the most commonly used reflector antennas.

5.1 EFFECTS OF DESIGN PARAMETERS ON THE SHAPE AND PATH LENGTH ERROR

To design the lens parameters (α, η, g, F) are required to be selected in such a way that the height of the feed contour and array contour are almost equal and the gap between the two contour remains minimum. The following guidelines are recommended to select the design parameters.

1. Select α = specified scanning angle.
2. Lens aperture Nmax is a function of antenna element spacing which controls the appearance of grating lobes.

   To Control the grating lobe, it is required that the antenna element spacing

   $d < \lambda / (2 + \sin \psi_m)$

   Where ψ_m is the maximum scanning angle and λ is the wavelength.
3. For minimum phase value "g" should be selected using the relation

   $g = 1+\alpha^2/2$ where $g = G / N_{max}$

For the dependency of phase error and shape of the lens, suitable value of "f" and "g" may be selected.

A Rotman lens is a three focal point lens. When feed is displaced from these focal points emitted wave-front will have phase error. Effects of design parameters on the path length error are described in chapter 2.

5.2 TWO DIMENSIONAL FIELD ANALYSIS OF THE LENS

Rotman lens is designed and analyzed using the software. The result of the analysis namely reflection coefficient, scattering matrix and radiation pattern of antenna array is presented. Result of the analysis verifies the guidelines to select the design parameters described in section 5.1.

The modified approach used to design the Rotman lens is known as Katagi lens. In this lens average percentage of power reflected back is large and power coupled back to the feed ports is small. The overall performance of Katagi lens is better than the Rotman lens.

Rotman types lens having Elliptical refocussed designed and analyzed using the software. Results of the analysis are compared with the result obtained from Rotman lens (proposed in chapter two). It is found that overall performance of Elliptical refocussed lens is better than Rotman lens.

Radiation pattern for all these lenses reveals are close as predicted by its design approach.

5.3 SUGGESTION FOR FUTURE WORK

For Rotman type bootlace lenses discussed so for it is necessary to investigate the following aspects to improve the performance of the lens.

Derivation of relations between lens parameters to minimize the path length error when other than elliptical focal arc is used.

REFERENCES

[1] Butler J. and Lowe R., "Beam forming matrix simplifies design of electronically scanned antennas," Electronics design 9, pp.170-173, 1961.

[2] W.Rotman and R.F.turner, "wide angle microwave lens for line source applications,"IEEE Trans. On Antennas & Propagation,Vol.Ap-11, pp. 623-632, Nov.1963.

[3] G. Larry Leonakis, "Correction to wide angle microwave lens for line source applications", IEEE Trans. On Antennas & Propagation, Vol.36, No.8, pp 1067 Aug.1986.

[4] J. Ruze, " Wide angle metal plate optics " Proc. IRE, vol.38, pp 53-59, Jan.1950.

[5] D. Archer, "Lens Fed multiple-beam arrays", Microwave J. Vol.18, pp 37-42, 1975.

[6] D. Archer, "Lens Fed multiple-beam arrays", Microwave J.Vol.18, pp. 171-195, Sept. 1984.

[7] J. Frank, "Bandwidth criterion for phased array antennas," Proceedings of phase array antenna symposium," Artech House, Dedham M.A.1972.

[8] T. Katagi, S. Mano and Shin-Lchi sato, "An improved design method of Rotman lens Antennas," IEEE Trans. on Antennas & Propagation, Vol.Ap-32, pp. 524-527, May 1984.

[9] J. P. Shelton, "Focusing characteristics of symmetrically configured bootlace Lenses," IEEE Trans. on Antennas & Propagation. Vol. AP-26, pp. 513-518, July 1978.

[10] M.S. Smith and A. K.S. Fong, "Amplitude performance of Ruze and Rotman lenses," The Radio and Electronic Engineer, Vol.53, pp.329-336, Sept.1983.

[11] Michel.J.Gans and Noach Amitay, "Narrow Multibeam Satellite ground Station Antenna Employing a Linear Array with a Geosynchronous Arc Coverage of 60 degree part II: Antenna Design," Antenna & propagation, IEEE Transaction on,Volume 31, Issue 6, pp.966-972, Nov.1983.

[12] Jeffrey S.Herd and David M.Pozar, " Design Of A Micro strip Antenna Array Fed By A Rotman Lens," Antenna & Propagation Society International Symposium, 1984,Volume 22 , pp. 729- 732, Jun 1984.

[13] C.M. Rappaport and A.I. Zaghloul, "Optimized three dimensional lenses for wide angle scanning," IEEE Tans. On Antenna and propagation, Vol. Ap.33, No.11, pp. 1227-1236, Nov. 1985.

[14] Hugh L. Southall and Daniel T.McGrawth, " An Experimental Completely Overlapped Subarray Antenna," Antennas And Propagation, IEEE Transaction on(legacy, pre-1988), Volume 34, Issue 4, pp. 465-474, April 1986.

[15] Deron L.Johnson, Michael J.Maybell and Joseph A.Troychak, "Octave Bandwidth, -35dB Sidelobe Single Offset Pillbox Reflector Using A Rotman Lens and Array as a Primary feed," Antenna & Propagation Society International Symposium, 1987, Volume 25, Jun. 1987.

[16] L.Musa,and M.Smith, " Microstrip Rotman lens port design" Antenna and propagation society international symposium,1986, volume 24, pp. 899-902, June 1986.

[17] L. Musa and M.S Smith, "Micro strip Port design and side wall absorption for printed Rotman lenses," Microwave, Antenna and propagation, IEE proceeding H, Volume 136, Issue 1, pp. 53-58, Feb.1989.

[18] D.R. Gagnon, "Procedure for correct refocusing of the Rotman lens according To Snell's law," IEEE Trans. On Antennas & Propagation, Vol.37, No.3, p.390-392, March 1989.

[19] M.C.D.Maddocks and M.S.Smith, "A Steerable flat plat antenna design for satellite Communication and broadcast reception," Antenna and Propagation, 1989, ICAP 89, Sixth International Conference, vol.1, pp. 40-44, 4-7 Apr 1989.

[20] K.K. Chan, "Planar waveguide model of Rotman lenses," On Antennas & Propagation, Society International Symposium,1989, AP-S Digest, Vol.2, pp. 651-654, 26-30 June1989.

[21] R.C.Hansen, "Design trades for rotmann lenses", IEEE Trans. On Antennas & Propagation, Vol. 39, No.4, pp. 464-472, April 1991.

[22] Leslie K.Jelalian and Ronald A. Gilbert, "A new design for a passive frequency Channelizer," Antenna & Propagation Society International Symposium, 1991, AP-S Digest, vol.1, pp.218-221, 24-28 June 1991.

[23] S.F.Peik, J.Heinstadt, "Multiple Beam Microstrip Array fed by Rotman Lens," Antennas and Propagation1995,. ICAP 95, Ninth International Conference on (Conf. No. 407), vol. 1, pp. 348-351, 4-7 April 1995.

[24] T. Katagi, S.Mano, S. Sato, P.K. Singhal and P.C .Sharma, "Comment on correction to an improved design method of Rotman lens Antennas," IEEE Trans. On Antennas & Propagation Vol. 43, No.6, p. 634. June1995.

[25] J.J.Lee, G.W.Valantine "Multibeam array using Rotman lens and RF Heterodyne" Antenna & Propagation Society International Symposium, 1990, AP-S. Digest, Vol. 3, 21-23 July 1996.

[26] Y.M. Tao and G.Y. Delisle, "Lens-Fed Multiple Beam array for millimeter wave Indoor communications," A&P Society International Symposium, 1997,IEEE Digest Volume 4, 13-18 July 1997.

[27] Ekkehart O. Rausch, Jay Sexton and Andrew F.Peterson, "Low Cost Compact Electrically Scanned Millimeter Wave Antenna," Aerospace and Electronics Conference, 1996, NAECON 1996, Proceeding of the IEEE 1996 National, Volume1, pp.41-47, 20-23 May 1996.

[28] E.O.Rausch, A.F.Peterson and W. Wiebach, " electronically scanned millimeter wave Antenna using a Rotman lens," Radar 97, (Conf. Publ. No.449), pp. 374-378, 14-16 Oct.1997.

[29] Ekkehart O. Rausch and Andrew F. Peterson and Wolfgang Wiebach, "Millimeter Wave Rotman Lens," Radar Conference,1997, IEEE National, pp.78-81, 13-15 May.1997.

[30] Phuong Phu, and James Lilly, "A Wide Band Width Electronic Scanning Antenna for Multimode RF Sensing,"Radar Conference 1999 IEEE, , pp. 177-180, 20-22 April 1999.

[31] P.K.Singhal, P.C.Sharma and R.D.Gupta, "Rotman Lens With Equal Height of Array and Feed Contours," IEEE Trans. On Antennas & Propagation Vol. 51, No.8, pp. 2048-2056. Aug. 2003.

[32] A.K.S.Fong and M.S. Smith, "A microstrip multiple beam forming lens," The radio and Electronic Engineer,Vol. 54, No.7/8, pp. 318-320, 1984.

[33] N.Yuan, J.S.Kot and A.J.Perfitt, "Analysys of Rotman lenses using a hybrid least squares FEM/transfinite element method," IEE Proc. Microwave, Antennas & Propagation Vol. 148, No.3, pp. 193-198. June 2001.

[34] P.C. Sharma ,K.C. Gupta, C.M.Tsai, J.D.Brice and R. Presnell, "Two-dimensional field analysis for CAD of Rotman type beam forming lenses," International J. of Microwave and Millimeter-Wave Computer Aided Engg. Vol.2, No.2, pp. 82-89, April 1992.

[35] P.K.Singhal, P.C.Sharma and R.D.Gupta, "Recent Trends in Design and Analysis of Rotman – Type Lens for Multiple Beamforming," International J.RF and Microwave Computer Aided Eng., Vol. CAE 8, pp. 321-338 1998.

[36] T. Okoshi, " Planar circuits for microwaves and light waves," Springer Series in Electrophysics, Vol.18, 1984.

[37] Y.Rahmat Samil, T.Itoh and R.Mitra, “A spectral domain analysis for solving Microstrip discontinuity problems,” IEEE Trans. on MTT, Vol-22, pp.372-378, April 1974.

[38] A.K.Sharma , “Spectral domain analysis of micro strip structures,” P.hd. dissertation, Deptt. Of Electrical Engg. ,I.I.T. New Delhi, India,1979

[39] T.Okoshi, T.Takeuchi and J.P.Hsu, “Planar 3-db hybrid circuit”, Electron Communication, Japan, Vol. 58-b, No.8, pp. 80-90, Aug.1975

[40] R.Chadha and K.C.Gupta, “Green’s functions for triangular segments in planar Microwave circuits,” IEEE Trans. On MTT, Vol.MTT-28, pp. 1139-1143, Oct. 1980.

[41] R.Chadha and K.C.Gupta, “Green’s functions for circulars sectors, annular rings and annular sectors in planar microwave circuits,” IEEE Trans. On MTT, Vol. MTT-29, pp. 68-71, Jan. 1981.

[42] T.Okoshi and T.Miyoshi, ”The planar circuit-an approach to microwave integrated Circuitry,” IEEE Trans. On MTT, Vol.MTT-20, pp. 245-252, April 1972.

[43] P. Silvester, “Finite element analysis of planar microwave networks,” IEEE Trans. on MTT,Vol.MTT-21, pp. 104-108, Feb. 1973.

List of Publications

1. DC Dhubkarya,P.K.Shinghal and R.C.Saraswat, "An overview of RF beam forming networks" Recent trends in Communication technology at Jiwaji University Gwalior during April 13-14,2002
2. DC Dhubkarya, P.K.Shinghal, "Comparison of the design approaches of Rotman type lens for multiple beam forming" IEEE International symposium on Antenna and Propagation at Seoul Korea on Aug.03-05,2005
3. DC Dhubkarya, P.K.Shinghal and R.C.Saraswat, "Elliptically focused lens for multiple beam forming" in InCMARS-2005 at ICRS Jodhpur on Dec.20-22,2005
4. DC Dhubkarya, P.K.Shinghal and R.C.Saraswat, " Design of equal height circular lens for multiple beam forming at UHF band" in InCMARS-2006 at ICRS Jodhpur on Dec.20-22,2006
5. DC Dhubkarya, P.K.Shinghal, RC Saraswat and R.P.S. Kushwah, "Comparative Analysis of WG & Microstrip Rotman lens," in InCMARS-2008 at ICRS Jodhpur on Feb.25-29,2008.